

Response to Anonymous Referee #1

To facilitate review of the referee comments, author responses, and substantial changes to the manuscript, we utilize the following scheme:

Referee comments

Author response

Text additions in block quotes

Text deletions in block quotes

Overview: I find this manuscript to be well written and logically organized. The manuscript describes particle chemical compositional changes measured downwind of two prescribed fire smoke plumes in SE US over 1.5 and 5 hours, respectively. As these measurements are difficult to obtain and there are very few such measurements reported in current literature, this manuscript is both timely and appropriate material for ACP. The manuscript should be published with attention paid to the following minor issues.

We thank the reviewer for these words of support and for the subsequent thoughtful comments, which we have addressed to the best of our ability.

1.) IE's given have units of "ions/molecule".

We thank the reviewer for this note and have added these units to the revised document.

2.) The paragraph about using no gas-phase correction in the AMS data analysis for CO₂ is incorrect and misleading. It needs to be removed or rewritten. The standard AMS analysis directly incorporates a standard CO₂ correction, as it is an important correction, in the fragmentation tables. Please see Allan et al., 2004. It is possible that the intent of the authors was to suggest that differences in gas phase CO₂ concentrations in and out of plume were insignificant, or that the constant pressure inlet reduced gas phase CO₂ concentrations below relevant signal levels, both of which might be true. However, since the authors present total OA, f44, and O:C measurements, all of which can be dramatically impacted by incorrect gas-phase CO₂ corrections, the authors need to clear this issue up.

We thank the reviewer for this comment. The speculation is correct: we did include the standard AMS analysis CO₂ correction but did not explicitly account for the measured CO₂ value. We have re-written this text as the following:

"While we obtained simultaneous measurements of gas-phase CO₂, we ~~have not corrected our data for any potential interference with the signal at m/z 44 (CO₂⁺) in the AMS~~ utilized the standard correction in the fragmentation table from Allan et al. (2004), rather than explicit corrections for CO₂ to account for differences within and without of the plume."

3.) In order to limit the size of this manuscript, Section 2.2.4 should be removed, unless the data in directly used in the manuscript, which I cannot seem to find.

We had originally included this description, since we presented some data in an earlier version of the manuscript derived from the AFTIR that indicated that the plume was photochemically active. We have since removed that figure but retained this text as it described complementary measurements collected during this campaign. Since both reviewers feel that this section is unnecessary, we have deleted the text for Section 2.2.4.

4.) In addition to (3) above, the discussion of Lagrangian or non-Lagrangian could be removed, as again while the data points are duly marked and the description and intent is clear, the differences in L or non-L data points appear to be never discussed or utilized in any way to suggest the differences are important. If the authors' decide to keep this in, then it would be important to at least describe how they differ or why they do not differ.

Our discussion of Lagrangian and non-Lagrangian is a remnant from earlier gas-phase analysis (e.g., Akagi et al., 2013) as this methodology provides some insight to downwind changes due to photochemistry and is not affected by dilution; however, this is complicated for the particle phase since dilution can induce evaporation. Hence, the distinction of data as "Lagrangian" or "non-Lagrangian" no longer has clear or relevant implications. Thus, we have deleted this paragraph and updated the figures accordingly.

5.) One must assume that the significance level assumed in the manuscript for the statistical tests is 0.05. It should be included.

We thank the reviewer for this comment as the assumed significance level is a critical piece of information that we mistakenly excluded from the submitted manuscript. To rectify this, we have added the following text to the second paragraph in the Results and Discussion section, which provides a basic overview of Figures 2-5 (e.g., what boxes and whiskers represent, how error bars were generated):

"To assess whether differences near the source and downwind are statistically significant, we conducted unpaired t-tests. When the corresponding two-tailed p value ≤ 0.05 , we consider the results to be significantly different; conversely, if the p value > 0.05 , we infer that there is no significant difference."

6.) Page 1968 line 22 appears to have the incorrect trend stated, which should read "f60 (Fig. 4c) is significantly lower downwind than at the source: : :"

We thank the reviewer for identifying this error, which has been corrected in the revised draft.

7.) Page 1970 line 10 "decrease" should be "increase".

We thank the reviewer for identifying this error, which has been corrected in the revised draft.

8.) The discussion of O:C and H:C in the same paragraph ends by comparing the trends in changing O:C and H:C downwind with the same trends that were demonstrated for thermal denuded OA. What is left unstated is that these same trends are also true for SOA formation. Can refer to Kroll et al., 2011. Thus, by chemical changes alone, this connection is a bit misleading. It needs to be paired with the decreasing OA loadings to suggest that dilution/evaporation may dominate. Part of the issue here is that the H:C typically goes down with increasing oxidation, as more H's are lost than C's, an explanation that was not included by the authors when attempting to describe why the H:C does not go up with dilution of higher H:C background aerosol.

We thank the reviewer for this comment, as our discussion was perhaps a bit misleading, or at the least, incomplete. We have added text to clarify and have paired this with the observed decrease in OA loading, per the reviewer's suggestion:

“For both fires, the average background H:C ratio was roughly 15% greater than the H:C at the source; downwind H:C values were mostly within the source variability. As the plumes were transported downwind and mixed with background OA, based on measured dilution rates we expected H:C to have increased toward the background values on a 2- to 3-hour timescale if it were a conserved tracer. The lack of a clear decrease increase with time since emission in both experiments suggests either that loss of both H and C occurred in the plume, or increases in C occurred without corresponding addition of H that would maintain the H:C observed at the source. Typically, H:C decreases with increasing oxidation (Heald et al., 2010).

For O:C, about half the downwind values were higher than could be explained by measured variability at the source, and the background OA had O:C within (but at the lower end) of the range at the source. Dilution with background air was thus expected to have had little impact on O:C if O:C were a conserved tracer. Like m/z 44, O:C could have increased with time if photochemical production and condensation of high O:C species or photochemical aging of aerosol had occurred (Kroll et al., 2011).

However, the observed decreases in $NEMR_{OA}$ (whether statistically significant or not) suggests that changes in H:C and O:C may potentially be induced by a solely physical process (i.e., if C were lost from the aerosol phase by preferential evaporation of species that had lower O:C than the average observed at the source). In fact, Huffman et al. (2009b) demonstrated that O:C increased and H:C decreased with increasing evaporation of bulk OA in biomass burning emissions during thermodenuder experiments. Hence, evaporative transformations may be difficult to differentiate from oxidative transformations.”

9.) Given the decrease in measured OA over the short time frames, it is definitely tempting to implicate dilution/evaporation over photochemical oxidation, though photochemical oxidation processes may also reduce the amount of OA in time. However, as the authors’ note, it is not necessarily clear how much of a role photochemical oxidation may have affected the observations. The authors give due time and effort to model the OA measurements as if dilution/evaporation was the only significant process in section 3.2. However, previous work by (some of) these authors reported observations of photochemical activity for these same biomass burning plumes (page 1967 lines 4-6). Why did the authors not try to at least quantify potential photochemical oxidation effects, especially if they might be predicted to be small?

We did, at one point, attempt to quantify these effects via a coupled gas-particle partitioning/ photochemistry box model to predict $NEMR_{OA}$, f_{60} , and f_{44} . Model results suggested that the upper bound prediction of SOA is roughly 30% of total excess OA after 5.5 hours. However, this result may be highly uncertain due to the required assumptions related to SOA precursor concentrations, SOA yields, inferred initial OH concentration, etc. Moreover, when testing this model against different data sets (from other airborne campaigns investigating biomass burning OA), it could not reproduce cases where the downwind $NEMR_{OA}$ increased (DeCarlo et al., 2008; Vakkari et al., 2014; Yokelson et al., 2009), so uncertainties and assumptions with this model appeared to be problematic. Ultimately, we decided to exclude this model and its results from our manuscript. Future work by Matt Alvarado and Chantelle Lonsdale will focus on the modeling of our OA data using the Aerosol Simulation Program (Alvarado and Prinn, 2009).

10.) Page 1972 line 14. “with decreasing plume-integrated COA” should probably read “with decreasing total measured (not background subtracted) COA”.

Per the reviewer’s suggestion, we have modified this text as follows:

“...with decreasing ~~plume-integrated~~ total measured (i.e., not background-corrected) C_{OA} ”

11.) Page 1973 lines 21-24. The authors switch from the discussion of how dilution/evaporation may dominate the biomass burning particle processes during downwind advection and appear to make a more concrete conclusion here and only here in the conclusions, suggesting that not only does the dilution-driven evaporation dominate over photochemical oxidation, but it happens in the first hour, after which the “OA in the plume reaches an equilibrium state with the background in our observations.” It is not clear where this additional information is presented in the results and discussion sections. On page 1967 at the end of section 3.0, the authors note that after 1.5 h from emission, no statistically-significant detectable change was observed in NEMR_OA for either of the two downwind burns. The authors’ should clearly discuss this statement, the associated uncertainties, and the underlying assumptions prior to the conclusions section.

We thank the reviewer for raising this issue since, as written, it lacks the clarification as stated in the comment.

“Our observations and model simulations suggest that dilution-driven evaporation out of the particle phase dominates over condensation of semi-volatile material into the particle phase over roughly the first two ~~one~~ hours of transport during the FJ 9b fire. ~~after which T~~ After this, the OA in the plume reached an apparent ~~equilibrium~~ steady-state with the background in our observations, as there is no net change to NEMR_{OA} (i.e., there is no obvious dilution-driven evaporation or SOA production); thus, OA can be predicted with a simple gas-particle partitioning model. For the Francis Marion fire, ~~due to limited downwind data~~, we cannot draw a similar conclusion ~~from the Francis Marion fire~~ with any certainty ~~due to limited downwind data~~.”

References

- Akagi, S. K., Yokelson, R. J., Burling, I. R., Meinardi, S., Simpson, I., Blake, D. R., McMeeking, G. R., Sullivan, A., Lee, T., Kreidenweis, S., Urbanski, S., Reardon, J., Griffith, D. W. T., Johnson, T. J. and Weise, D. R.: Measurements of reactive trace gases and variable O₃ formation rates in some South Carolina biomass burning plumes, *Atmos. Chem. Phys.*, 13(3), 1141–1165, doi:10.5194/acp-13-1141-2013, 2013.
- Alvarado, M. J. and Prinn, R. G.: Formation of ozone and growth of aerosols in young smoke plumes from biomass burning: 1. Lagrangian parcel studies, *J. Geophys. Res.*, 114(D9), D09306, doi:10.1029/2008JD011144, 2009.
- DeCarlo, P. F., Dunlea, E. J., Kimmel, J. R., Aiken, A. C., Sueper, D., Crouse, J., Wennberg, P. O., Emmons, L., Shinozuka, Y., Clarke, A., Zhou, J., Tomlinson, J., Collins, D. R., Knapp, D., Weinheimer, A. J., Montzka, D. D., Campos, T. and Jimenez, J. L.: Fast airborne aerosol size and chemistry measurements above Mexico City and Central Mexico during the MILAGRO campaign, *Atmos. Chem. Phys.*, 8(14), 4027–4048, doi:10.5194/acp-8-4027-2008, 2008.
- Heald, C. L., Kroll, J. H., Jimenez, J. L., Docherty, K. S., DeCarlo, P. F., Aiken, A. C., Chen, Q., Martin, S. T., Farmer, D. K. and Artaxo, P.: A simplified description of the evolution of organic aerosol composition in the atmosphere, *Geophys. Res. Lett.*, 37(8), L08803, doi:10.1029/2010GL042737, 2010.

Huffman, J. A., Docherty, K. S., Mohr, C., Cubison, M. J., Ulbrich, I. M., Ziemann, P. J., Onasch, T. B. and Jimenez, J. L.: Chemically-Resolved Volatility Measurements of Organic Aerosol from Different Sources, *Environ. Sci. Technol.*, 43(14), 5351–5357, doi:10.1021/es803539d, 2009.

Kroll, J. H., Donahue, N. M., Jimenez, J. L., Kessler, S. H., Canagaratna, M. R., Wilson, K. R., Altieri, K. E., Mazzoleni, L. R., Wozniak, A. S., Bluhm, H., Mysak, E. R., Smith, J. D., Kolb, C. E. and Worsnop, D. R.: Carbon oxidation state as a metric for describing the chemistry of atmospheric organic aerosol., *Nat. Chem.*, 3(2), 133–9, doi:10.1038/nchem.948, 2011.

Vakkari, V., Kerminen, V.-M., Beukes, J. P., Tiitta, P., van Zyl, P. G., Josipovic, M., Venter, A. D., Jaars, K., Worsnop, D. R., Kulmala, M. and Laakso, L.: Rapid changes in biomass burning aerosols by atmospheric oxidation, *Geophys. Res. Lett.*, 41(7), 2644–2651, doi:10.1002/2014GL059396, 2014.

Yokelson, R. J., Crouse, J. D., DeCarlo, P. F., Karl, T., Urbanski, S., Atlas, E., Campos, T., Shinozuka, Y., Kapustin, V., Clarke, A. D., Weinheimer, A., Knapp, D. J., Montzka, D. D., Holloway, J., Weibring, P., Flocke, F., Zheng, W., Toohey, D., Wennberg, P. O., Wiedinmyer, C., Mauldin, L., Fried, A., Richter, D., Walega, J., Jimenez, J. L., Adachi, K., Buseck, P. R., Hall, S. R. and Shetter, R.: Emissions from biomass burning in the Yucatan, *Atmos. Chem. Phys.*, 9(15), 5785–5812, doi:10.5194/acp-9-5785-2009, 2009.

Response to William Morgan

To facilitate review of the referee comments, author responses, and substantial changes to the manuscript, we utilize the following scheme:

Reviewer comments

Author response

Text additions in block quotes

Text deletions in block quotes

The manuscript is well written and adds to the relatively scarce number of observations of fresh smoke plumes and their subsequent evolution. This is a timely and helpful addition to the literature, given the somewhat conflicting nature of previous observations. The manuscript adds insights into the potential drivers of the transformation of organic aerosol in the initial stages of smoke plume evolution, which is appropriate for ACP. The manuscript is suitable for publication once some issues with the data analysis have been cleared up and some minor issues have been addressed.

We thank the reviewer for his praise of our manuscript and thoughtful comments, which we have addressed individually below.

P1955, L19-20: The authors suggest that ‘increases in f44 are typically interpreted as indicating chemical production of SOA’ – I would say that typically, increases in f44 are thought to ‘typically’ indicate aging of SOA, rather than formation. It can be indicative of formation. I would suggest clarifying the text here.

Per the reviewer’s suggestion, we have replaced “production” with “aging”.

P1957, L21-26: Is it really necessary to say that this is the first study to use that combination of instruments, especially when most of them have little or no use in this manuscript? If it is necessary, a sentence to illustrate why would be useful. At the moment it just seems like unnecessary boasting.

We have modified the text to read “The SCREAM campaign combined simultaneous aircraft...”

Section 2.1: It would be useful to include the typical altitudes for the sampling e.g. at what altitude was the close-to-source sampling conducted and what altitude was the downwind sampling conducted? Approximately how old was the initial smoke that was sampled close-to-source? This is useful context for both this manuscript and future studies that will likely cite this work.

The reviewer raises two valid points in this comment, both of which we have addressed in the text. To respond to the first point, we moved from Section 2.3 to Section 2.1 with text related to smoke age added for clarification, while the response to the latter point is a combination of text moved from Section 2.3 and additional text added for clarification.

On smoke age we added:

“For consistency with May et al. (2014), we defined “near-source” samples as those collected within 5 km of the fire (always less than 30 minutes of aging, but most of the smoke had an age < 10 minutes based on average ambient wind speed), while downwind samples were those collected at distances greater than 5 km.”

On sampling altitude we clarify:

“The first 1-2 hours of flight time was typically spent sampling near the source at ~100-600 m altitude. Following this characterization period, it was possible to sample smoke downwind with 1-2 hours of atmospheric aging, so we then alternated downwind cross-plume samples with occasional additional source sampling. A challenge was that emissions were rapidly diluted and mixed within the boundary layer (within roughly 30 min downwind), and the plumes did not penetrate into the free troposphere, so visual tracking of the plumes was difficult. In fact, the flight path was guided via consultation with real-time instrument output, which enabled the identification of plume center and extent as well as the marking of way points. Furthermore, the plume from the FJ 22b fire entered restricted air space near Columbia, SC, so it was only possible to follow this plume for a short distance from the point of emission.

Downwind, the Twin Otter typically flew at altitudes between 500 m and 1500 m, but not with sufficient detail to develop vertical profiles. All data, regardless of sampling altitude (or latitude/longitude), are categorized as “within the plume” or “outside of the plume” along with the additional distinction of “estimated time since emission” (please refer to Section 2.3.1).”

P1960, L6: What does ‘adjusted’ mean in this context? Was the data simply averaged to the AMS time base or were the time series shifted to account for differences in inlet and/or instrument lag times? If so, how was this done?

In our analysis, we adjusted times via the latter approach suggested by the reviewer and subsequently integrated the peaks; we did not average any data to the AMS time base. We have noted this change in the text:

“For consistency, all data were adjusted to the same timestamp via alignment of peaks (thus accounting for differences in both instrument clocks and instrument response times), which we defined from HR-ToF-AMS.”

Section 2.2.1: The uncertainties relating to the AMS collection efficiency (CE) should be expanded on here and a discussion of how they may affect the latter analysis should be included.

It is not clear how appropriate the Middlebrook et al. CE calculator is for aerosol that is dominated by organic material (such as biomass burning). As the authors are aware, there is a large range of AMS CE values (approx. 0.5 to 1.0) reported in the literature for biomass burning aerosol, which can introduce an additional uncertainty of a factor of two. Was an external measurement available during SCREAM that could be used to validate the AMS CE calculation? Furthermore, do the authors have any insights from their prior biomass burning datasets that may help to validate the use of this procedure?

As the reviewer states, there is a large range of AMS CE reported for biomass burning aerosol. Unfortunately, there was no external measurement available that might validate our AMS CE calculation as the only instruments deployed on the aircraft were an AMS, an SP2, an AFTIR, and a fraction collector for water-soluble compounds.

Rather than assume a value based on literature, we elected to utilize the empirical calculator. Furthermore, in these samples, we are dealing with both in-plume and out-of-plume aerosol. While the CE for biomass burning emissions (as derived from laboratory data) may vary from 0.5 to 1.0 based on the literature (Hennigan et al., 2011; Heringa et al., 2011; Weimer et al., 2008), the general consensus for ambient aerosol is a CE = 0.5. Since the smoke plumes are mixing with ambient air, it is likely that the

CE will evolve over time due to the mixing of smoke aerosol with regional background aerosol. Hence, we feel that calculating CE is more appropriate than applying different CE to in-plume and out-of-plume data.

To address the potential uncertainty of an “unvalidated” CE based on the Middlebrook et al. (2012) calculator, we have added a similar line of text to that in the May et al. (2014) paper which focused solely on primary emissions from this aircraft campaign (as well as another aircraft campaign and a laboratory campaign):

“As stated in May et al. (2014), our results are potentially biased by up to a factor of two due to the inherent uncertainty in our estimation of CE.”

The authors refer to May et al. (2014) for further details regarding the AMS data quality assurance for the inorganic species and I see that they have made fairly typical adjustments to the fragmentation table for nitrate and sulphate ions. Given that the Middlebrook et al. CE calculator evaluates the CE depending on the contribution of the inorganic species, I wonder how much impact any composition changes in the plumes downwind will impact on the CE? Does nitrate form in the plumes downwind and does this impact the CE? Does the acidity of the aerosol evolve downwind (this requires careful and uncertain analysis of the ammonium contribution also, which is challenging for biomass burning aerosol with the AMS)? Discussion of these issues is required and how the uncertainty in the CE may impact the reported significance of the observed trends downwind should be included in the revised manuscript.

While the reviewer raises very good points in this comment, we cannot fully respond to these points in the revised manuscript. We have made no attempts to quantify the evolution of aerosol acidity. At one point, we did attempt to investigate nitrate aerosol formation downwind for comparison with AMS data as part of a modeling study focused on gas-phase chemistry, but this never progressed beyond preliminary efforts. Ultimately, we chose to focus solely on OA for this work.

However, as the reviewer notes, changes in composition downwind may impact the CE, which further supports our choice of using the composition-dependent CE calculator, as this likely provides a more robust estimate than the arbitrary assumption that $CE = 0.5$ or $CE = 1$, based on prior work.

P1961, L1: Clarify that with no particle time-of-flight data being collected, no size resolved information is available from the AMS.

We have added this clarification per the reviewer’s suggestion as follows:

“During operation, data were exclusively collected using the “V-mode” of the ion time-of-flight within the mass spectrometer; since no particle time-of-flight data were collected, no size-resolved information is available.”

P1961, L3-L11: As noted by Referee #1, this is misleading regarding the CO₂ correction for the AMS.

As described in the response to Referee #1, we have modified this text as follows:

“While we obtained simultaneous measurements of gas-phase CO₂, we ~~have not corrected our data for any potential interference with the signal at m/z 44 (CO₂⁺) in the AMS~~ utilized the standard correction in

the fragmentation table from Allan et al. (2004), rather than explicit corrections for CO₂ to account for differences within and without of the plume.”

Section 2.2.4: As noted by Referee #1, is this section necessary?

As noted in the response to Referee #1, we have removed this text.

P1966, L15: Is it appropriate to call these ‘Lagrangian’? This assumes that the fire characteristics and emissions are fixed over the time span between sampling the initial smoke and its subsequent evolution downwind. Do the measurements support this (the manuscript suggests not on P1966, L25)? Just flying along the plume does not guarantee this given that the speed of the aircraft and the speed by which the smoke is transported is not synchronised. I would suggest changing the terminology here or better defending this classification.

The discussion of Lagrangian versus non-Lagrangian originally followed the discussion of the gas-phase data presented in Akagi et al. (2013). However, based on the reviewer comments and discussion among co-authors, we no longer feel that this distinction is appropriate. We have deleted the paragraph in question and have updated figures accordingly.

P1967, L25-28: This framework was also demonstrated in a partner paper to the Ng et al. (2010) paper in Morgan et al. (2010), which should be referenced here. The reference is included below.

Morgan, W. T., Allan, J. D., Bower, K. N., Highwood, E. J., Liu, D., McMeeking, G. R., : : : Coe, H. (2010). Airborne measurements of the spatial distribution of aerosol chemical composition across Europe and evolution of the organic fraction. *Atmospheric Chemistry and Physics*, 10(8), 4065–4083. <http://doi.org/10.5194/acp-10-4065-2010>.

We have added the reviewer’s reference.

P1968, L2: This is a somewhat confusing definition of f₄₄ for those unfamiliar with the AMS, as it suggests that C₄₄ is the mass concentration of particulate CO₂⁺. While this is correct as far as the AMS fragmentation pattern is concerned, the CO₂⁺ particulate signal is thought to arise due to decarboxylation on the vaporiser surface, rather than carbon dioxide being present in the actual aerosol sample. This should be clarified in the revised manuscript.

Per the reviewer’s suggestion, we have modified the text in question as follows:

“C₄₄ is the mass concentration of particulate CO₂⁺, which is likely due to decarboxylation on the vaporizer surface rather than CO₂ molecules being present in the aerosol sample”

Figure 1: I suggest using a more colour-blind friendly scale on these flight tracks. Panel a) is particularly difficult to judge the differences. Color Brewer (<http://colorbrewer2.org/>) is a very useful resource for colour-blind friendly scales.

We have modified the color scale in this figure to a “yellow-hot” scheme rather than “rainbow” that appears to be color-blind friendly. If our new scheme is still problematic, we encourage the reviewer to follow up with us regarding this.

Figure 2: There is a seemingly large variation in the emission factors for CO and CO₂ in these figures. What do the authors attribute this to and how does it affect the interpretation of the results?

The total variation in EF_{CO_2} is only about 5%, but the total variation in EF_{CO} is closer to 50%. Since the EF_{CO} values should ideally be conserved with aging, the variation in EF_{CO} likely arises from three sources: a) lower S:N in the excess CO measurement by CRDS for CO than for CO₂, b) imperfect mixing of the source smoke so that even pseudo-Lagrangian (retaining this argument here since it is applicable to gas-phase data) samples can be impacted to some extent by spatial variability in smoke composition near the source, or c) excess CO₂ values (10s of ppmv) that are small compared to the background (~400 ppmv). Since OA and CO emissions are both from smoldering and should be somewhat correlated, the lack of correlation between the NEMR for OA/CO and EF_{CO} suggests the variation is mainly the higher noise in the CO measurement. The average downwind value is not significantly different from the source average so no bias is indicated. It is possible that source variability is larger than indicated by the box-whisper plot, but those measurements were made at higher concentrations with more S:N than downwind so we have retained the estimate of source variability based on source samples in our analysis. However, given that only the reported EF have substantial noise (e.g., Figure 2c-d, Figure 3c-d, Figure 6), we speculate that argument c) may be the primary driver of this variability. Ultimately, we do not feel that these variations affect our interpretation of results.

Figure 6: There appears to be significant overlap between the near-source and downwind data for FJ 9b and Francis Marion fires. What do the authors attribute this to? As noted previously, it would be useful to include more details regarding the near-source samples.

The overlap to which the reviewer has referred is also apparent in Figures 2 and 3. Based on these figures, it is likely that the largest factor contributing to this is source variability. For example, the interquartile range for the FJ 9b fire is roughly $10 \mu\text{g m}^{-3} \text{ppmv-CO}^{-1}$ while it is roughly $15 \mu\text{g m}^{-3} \text{ppmv-CO}^{-1}$ for the Francis Marion fire. Furthermore, our statistical test suggests that there is no significant difference between the near-source and downwind NEMR_{OA} data for the Francis Marion fire, so it is not surprising that when converted to OA concentration, these data overlap.

The sampling details do contribute to this figure showing OA loading and the corresponding emission factor. The main point of this figure is that on average, a laboratory-derived parameterization of the impact of dilution on the gas-particle partitioning can reproduce the EF_{OA} observed for real-world (prescribed) fires, within measurement/model uncertainty, for both near-source and downwind data at different loadings. Variability in near-source data arises due to proximity to the source and to the center of the plume as well as the smoke production rate.

References:

Akagi, S. K., Yokelson, R. J., Burling, I. R., Meinardi, S., Simpson, I., Blake, D. R., McMeeking, G. R., Sullivan, A., Lee, T., Kreidenweis, S., Urbanski, S., Reardon, J., Griffith, D. W. T., Johnson, T. J. and Weise, D. R.: Measurements of reactive trace gases and variable O₃ formation rates in some South Carolina biomass burning plumes, *Atmos. Chem. Phys.*, 13(3), 1141–1165, doi:10.5194/acp-13-1141-2013, 2013.

Hennigan, C. J., Miracolo, M. A., Engelhart, G. J., May, A. A., Presto, A. A., Lee, T., Sullivan, A. P., McMeeking, G. R., Coe, H., Wold, C. E., Hao, W.-M., Gilman, J. B., Kuster, W. C., de Gouw, J., Schichtel, B. A., Kreidenweis, S. M. and Robinson, A. L.: Chemical and physical transformations of

organic aerosol from the photo-oxidation of open biomass burning emissions in an environmental chamber, *Atmos. Chem. Phys.*, 11(15), 7669–7686, doi:10.5194/acp-11-7669-2011, 2011.

Heringa, M. F., DeCarlo, P. F., Chirico, R., Tritscher, T., Dommen, J., Weingartner, E., Richter, R., Wehrle, G., Prévôt, A. S. H. and Baltensperger, U.: Investigations of primary and secondary particulate matter of different wood combustion appliances with a high-resolution time-of-flight aerosol mass spectrometer, *Atmos. Chem. Phys.*, 11(12), 5945–5957, doi:10.5194/acp-11-5945-2011, 2011.

May, A. A., McMeeking, G. R., Lee, T., Taylor, J. W., Craven, J. S., Burling, I., Sullivan, A. P., Akagi, S., Collett, J. L., Flynn, M., Coe, H., Urbanski, S. P., Seinfeld, J. H., Yokelson, R. J. and Kreidenweis, S. M.: Aerosol emissions from prescribed fires in the United States: A synthesis of laboratory and aircraft measurements, *J. Geophys. Res. Atmos.*, 119(20), 11,826–11,849, doi:10.1002/2014JD021848, 2014.

Middlebrook, A. M., Bahreini, R., Jimenez, J. L. and Canagaratna, M. R.: Evaluation of Composition-Dependent Collection Efficiencies for the Aerodyne Aerosol Mass Spectrometer using Field Data, *Aerosol Sci. Technol.*, 46(3), 258–271, doi:10.1080/02786826.2011.620041, 2012.

Weimer, S., Alfarra, M. R., Schreiber, D., Mohr, M., Prévôt, A. S. H. and Baltensperger, U.: Organic aerosol mass spectral signatures from wood-burning emissions: Influence of burning conditions and wood type, *J. Geophys. Res.*, 113(D10), D10304, doi:10.1029/2007JD009309, 2008.

1 Observations and Analysis of Organic 2 Aerosol Evolution in Some Prescribed Fire 3 Smoke Plumes

4 A.A. May^{1,2*}, T. Lee^{1,3}, G.R. McMeeking^{1,4}, S. Akagi⁵, A.P. Sullivan¹, S. Urbanski⁶, R.J.

5 Yokelson⁵, S.M. Kreidenweis^{1*}

6 1 Department of Atmospheric Science, Colorado State University, Fort Collins, CO, USA

7 2 Now with Department of Civil, Environmental and Geodetic Engineering, The Ohio State

8 University, Columbus, OH, USA

9 3 Now with Department of Environmental Science, Hankuk University of Foreign Studies,

10 Yongin, Korea

11 4 Now with Droplet Measurement Technologies, Boulder, CO, USA

12 5 Department of Chemistry, University of Montana, Missoula, MT, USA

13 6 Missoula Fire Sciences Laboratory, Rocky Mountain Research Station, US Forest Service,

14 Missoula, MT, USA

15 * Corresponding authors: A.A. May, may.561@osu.edu; S.M. Kreidenweis,

16 sonia@atmos.colostate.edu

17

18 Abstract

19 Open biomass burning is a significant source of primary air pollutants such as particulate matter
20 (PM) and non-methane organic gases (NMOG). However, the physical and chemical
21 atmospheric processing of these emissions during transport is poorly understood. Atmospheric
22 transformations of biomass burning emissions have been investigated in environmental
23 chambers, but there have been limited opportunities to investigate these transformations in the
24 atmosphere. In this study, we deployed a suite of real-time instrumentation on a Twin Otter
25 aircraft to sample smoke from prescribed fires in South Carolina, conducting measurements at
26 both the source and downwind to characterize smoke evolution with atmospheric aging. Organic
27 aerosol (OA) within the smoke plumes was quantified using an Aerosol Mass Spectrometer
28 (AMS), along with refractory black carbon (rBC) using a Single Particle Soot Photometer and
29 carbon monoxide (CO) and carbon dioxide (CO₂) using a Cavity Ring-Down Spectrometer.
30 During the two fires for which we were able to obtain aerosol aging data, normalized excess
31 mixing ratios and “export factors” of conserved species (rBC, CO, CO₂) ~~were~~
32 ~~unchanged~~ suggested that changes in emissions at the source did not account for most of the
33 differences observed in samples ~~with~~ of increasing ~~sample~~ age. Investigation of AMS mass
34 fragments indicated that the in-plume fractional contribution ($f_{m/z}$) to OA of the primary fragment
35 (m/z 60) decreased downwind, while the fractional contribution of the secondary fragment (m/z
36 44) increased. Increases in f_{44} are typically interpreted as indicating chemical ~~production~~ aging of
37 ~~secondary~~ OA (~~SOA~~). Likewise, we observed an increase in the O:C elemental ratio downwind,
38 which is usually associated with aerosol aging. However, the rapid mixing of these plumes into
39 the background air suggests that these chemical transformations may be attributable to the
40 different volatilities of the compounds that fragment to these m/z in the AMS. The gas-particle

41 partitioning behavior of the bulk OA observed during the study was consistent with the
42 predictions from a parameterization developed for open biomass burning emissions in the
43 laboratory. Furthermore, we observed no statistically-significant increase in total organic mass
44 with atmospheric transport. Hence, our results suggest that dilution-driven evaporation likely
45 dominated over chemical production of SOA within our smoke plumes, likely due to the fast
46 dilution and limited aging times ($< \sim 5$ hr) that we could sample.

47 1. Introduction

48 Open biomass burning is estimated to be the largest contributor on a global scale to
49 atmospheric fine carbonaceous particulate matter (PM) (Bond et al., 2013) and the second largest
50 contributor to atmospheric non-methane organic gases (NMOG) (Akagi et al., 2011). Substantial
51 research has been focused on characterizing gas- and particle-phase primary emissions from
52 biomass burning and the development of emission inventories (Akagi et al., 2011; Burling et al.,
53 2010, 2011; Christian et al., 2003; Hosseini et al., 2013; May et al., 2014; McMeeking et al.,
54 2009; Reid et al., 2005; Urbanski, 2013; Urbanski et al., 2011; Watson et al., 2011; van der Werf
55 et al., 2010; Wiedinmyer et al., 2006, 2011; Yokelson et al., 2013a). These emissions are
56 ultimately integrated into chemical transport models used to predict regional air quality and
57 global climate impacts.

58 Organic aerosol (OA) species represent the major component by mass in the submicron
59 carbonaceous PM emitted from fires (May et al., 2014; McMeeking et al., 2009; Reid et al.,
60 2005). In general, the physical and chemical evolution of biomass-burning-derived OA in the
61 atmosphere after emission is poorly understood, in part ~~since~~because OA is a “metastable
62 intermediate” (Donahue et al., 2013). Since OA consists of thousands of species with a spectrum
63 of temperature-dependent saturation vapor pressures, the portion of OA that is observable as PM

64 varies with dilution and with atmospheric temperature. Further, many of the species comprising
65 OA have been shown to undergo oxidation reactions, forming secondary products with their own
66 range of volatilities. In field studies, OA in biomass burning plumes has been observed to be
67 enhanced, be depleted, or remain constant with time after emission (Akagi et al., 2012; Capes et
68 al., 2008; Cubison et al., 2011; DeCarlo et al., 2008; Jolleys et al., 2012; Vakkari et al., 2014;
69 Yokelson et al., 2009), but due to the complexities described above, attribution of these
70 transformations to specific physical and chemical processes is difficult (Heilman et al., 2014).

71 Laboratory studies have been conducted to attempt to separate these processes for
72 biomass-burning-derived OA. As part of the third Fire Lab at Missoula Experiment (FLAME-
73 III), May et al. (2013) derived a volatility distribution and related thermodynamic parameters
74 representative of the primary emissions from all of the biomass fuels studied. In that same study,
75 Hennigan et al. (2011) and Ortega et al. (2013) investigated chemical transformations of the
76 emissions using an environmental chamber and a potential aerosol mass chamber, respectively.
77 Results from both chambers demonstrated that the OA mass can be enhanced, depleted, or
78 remain roughly constant with oxidation, similar to field measurements, yet the OA [always](#)
79 became apparently more oxidized with photochemical aging, as interpreted from the organic
80 mass fragments measured via online aerosol mass spectrometry.

81 In this work, we report and interpret observations from the South Carolina fiRe
82 Emissions And Measurements (SCREAM) campaign conducted in October-November 2011
83 (Akagi et al., 2013, 2014; May et al., 2014; Sullivan et al., 2014). The objectives of SCREAM
84 were to: [\(1\)](#) simulate moderately intense wildfires by conducting prescribed burns at sites with
85 high fuel loadings, ~~to~~ [\(2\)](#) characterize the emissions and develop estimates of emission factors
86 and emission ratios from both ground- and aircraft-based sampling, and [\(3\)](#) ~~to~~ sample plumes

87 downwind as they evolved during atmospheric transport. We also sampled fires of opportunity
88 during the study. The SCREAM campaign ~~was the first study, to our knowledge, to~~
89 ~~include~~ combined simultaneous aircraft-based online measurements of refractory black carbon
90 (rBC), time-resolved non-refractory sub-micron PM measurements (including OA), and time-
91 resolved water-soluble organic carbon (WSOC) and levoglucosan (LEV) measurements; in
92 addition to a suite of gas-phase compounds. Companion papers have reported airborne trace gas
93 emissions (Akagi et al., 2013), ground-based trace gas emissions (Akagi et al., 2014), airborne
94 WSOC and smoke marker emissions (Sullivan et al., 2014), and airborne primary PM emissions
95 (May et al., 2014). This paper focuses on airborne observations of the OA mass concentrations
96 and composition near the source and transformations to OA mass concentration and composition
97 during the first hours of atmospheric transport.

98 2. Methods

99 Emissions from five of the seven fires sampled during SCREAM are discussed in this paper.
100 Details including fuel type, area burned, meteorology and stand history were provided by Akagi
101 et al. (2013) and are summarized briefly here. Two of the burns were conducted on the Fort
102 Jackson (FJ) Army Base (located northeast of Columbia, SC) in Blocks 9b (FJ 9b; 34°0'15" N,
103 80°52'37" W; 1 November 2011) and 22b (FJ 22b; 34°5'4" N, 80°52'16" W; 2 November 2011).
104 These burns occurred in older stands that had not been treated for a number of years, and were
105 intended to simulate wildfires. Fuel inventories indicated that [the](#) vegetation comprised primarily
106 [of](#) mature longleaf pine (*Pinus palustris*) and loblolly pine (*Pinus taeda*) with some contributions
107 of turkey oak (*Quercus laevis* Walter) and farkleberry (*Vaccinium arboretum* Marsh.).
108 Complementary ground-based measurements of emissions from the FJ burns were reported by

109 Akagi et al. (2014). The three other sampled fires were designated Georgetown (33°12'9" N,
110 79°24'6" W; 7 November 2011), Francis Marion (33°12'55" N, 79°28'34" W; 8 November
111 2011), and Bamberg (33°14'5" N, 80°56'41" W; 10 November 2011), based on the location in
112 SC where the fire occurred. Georgetown and Francis Marion were located in coastal SC, likely
113 burning coastal grasses and longleaf pine understory, respectively, based on in-flight
114 observations. The Bamberg fire, located roughly 80 km due south of the Fort Jackson site in
115 inland SC, was likely comprised of multiple fuel types, including longleaf/loblolly pine
116 understory as well as marsh grasses, based on smoke marker ratio measurements reported in
117 Sullivan et al. (2014).

118 2.1. Sample Collection

119 Smoke plumes during SCREAM were sampled via airborne measurements onboard a United
120 States Forest Service DHC-6 Twin Otter aircraft. Sampling strategies and flight tracks are
121 described in prior literature from the SCREAM study (Akagi et al., 2013; May et al., 2014;
122 Sullivan et al., 2014). Fires were initiated in mid-morning, and the aircraft initially sampled the
123 emissions near the source. Following the source characterization period, the downwind plume
124 was sampled to investigate the effect of chemical and physical aging during atmospheric
125 transport. For consistency with May et al. (2014), we defined “near-source” samples as those
126 collected within 5 km of the fire (always less than 30 minutes of aging, but most of the smoke
127 had an age of < 10 minutes based on average ambient wind speed), while downwind samples
128 were those collected at distances greater than 5 km. During flights, there were also periods of
129 out-of-plume background sampling to establish time-dependent background concentrations of
130 the species that were quantified in the plume.

131 _____ The flight path for the FJ 9b burn is provided in Figure 1 as one example. Figure 1a
132 provides total (i.e., not background-corrected) OA mass concentration (C_{OA}), which was

133 typically between 3-7 $\mu\text{g m}^{-3}$ (average = 4.6 $\mu\text{g m}^{-3}$) outside of the plume throughout the
134 sampling domain, with the exception of ~~a band of data collected to the southwest of the fire~~
135 ~~source~~ higher concentrations that is attributable to the smoke plume. Correcting the data for the
136 background OA results in Figure 1b; here, the plume transport is more distinct.

137 The first 1-2 hours of flight time was typically spent sampling near the source at ~100-
138 600 m altitude. Following this characterization period, it was possible to sample smoke
139 downwind with 1-2 hours of atmospheric aging, so we then alternated downwind cross-plume
140 samples with occasional additional source sampling. A challenge was that ~~E~~missions were
141 rapidly diluted and mixed within the boundary layer (~~within roughly 30 min downwind~~), and the
142 plumes did not penetrate into the free troposphere, so visual tracking of the plumes was
143 challenging. In fact, the flight path was guided via consultation with real-time instrument output,
144 which enabled the identification of plume center and extent as well as the marking of way points.
145 Furthermore, the plume from the FJ 22b fire entered restricted air space near Columbia, SC, so it
146 was only possible to follow this plume for a short distance from the point of emission.

147 During flights ~~Downwind~~, the Twin Otter typically flew at altitudes between 500 m and
148 1500 m, but not with sufficient detail to ~~. However, as with flight pathes, sampling elevation was~~
149 ~~not systematic in nature, and we have made no attempt to~~ develop vertical profiles. All data,
150 regardless of sampling altitude (or latitude/longitude), are categorized as “within the plume” or
151 “outside of the plume” along with the additional distinction of “estimated time since emission”
152 (please refer to Section 2.3.1).

153 2.2. Instrumentation

154 The instrumentation installed on the Twin Otter used to characterize emissions included a
155 High-Resolution Time-of-Flight Aerosol Mass Spectrometer (HR-ToF-AMS; Aerodyne

156 Research, Inc.), a Single Particle Soot Photometer (SP2; Droplet Measurement Technologies,
157 Inc.), a Cavity Ring-Down Spectrometer (CRDS; Picarro G2401; Picarro, Inc.), an airborne
158 Fourier-transform infrared spectrometer (AFTIR), a Particle-into-Liquid Sampler/Total Organic
159 Carbon and fraction collector system (Sullivan et al., 2014) and an Aircraft Integrated
160 Meteorological Measuring System (AIMMS-20) probe (Aventech Research, Inc.). The AIMMS-
161 20 provided meteorological data such as three-dimensional wind vectors, three-dimensional
162 position of the aircraft (i.e., latitude, longitude, and altitude), ambient temperature, and ambient
163 relative humidity. All sampling was conducted from a low turbulence inlet (Wilson et al., 2004)
164 followed by a non-rotating Micro Orifice Uniform Deposit Impactor (MOUDI; Marple et al.,
165 1991). The MOUDI was operated such that it served as a PM₁ ~~impactor-selector~~ (i.e., having
166 50% particle transmission efficiency for particulate matter of 1 μm aerodynamic diameter with a
167 sharpness of 1.08 – particles less than roughly 900 nm will be transmitted with 100% efficiency).
168 ~~For consistency, a~~All data were adjusted to the same timestamp via alignment of peaks (thus
169 accounting for differences in both instrument clocks and instrument response times), which we
170 ~~defined from~~referenced to the HR-ToF-AMS.

171 2.2.1. Aerosol Mass Spectrometer

172 The HR-ToF-AMS (hereafter AMS) characterizes non-refractory sub-micron aerosol by
173 focusing sampled particles through an aerodynamic lens, collecting particles on a thermal
174 vaporizer, ionizing the vaporized particles via electron impaction, and detecting ions (m/z) in the
175 high-resolution time-of-flight mass spectrometer (DeCarlo et al., 2006). Using the ToF-AMS
176 data analysis toolkit SQUIRREL/PIKA (Sueper et al., 2013), aerosol mass concentrations can be
177 reconstructed from the m/z signal; for this study, we fit HR peaks for $m/z \leq 200$. These
178 concentrations are dependent on instrument parameters (e.g., ionization efficiency and vaporizer
179 collection efficiency). Ionization efficiency calibrations were performed with 350 nm ammonium

180 nitrate particles throughout the campaign, with values ranging from 1.83×10^{-7} to 2.91×10^{-7} ions
181 molecule⁻¹. Composition-dependent collection efficiencies were calculated following the
182 algorithm of Middlebrook et al. (2012), which is now built into the SQUIRREL software, for
183 each AMS sample and ranged from roughly 0.5-0.9, with a campaign-average value of 0.53. We
184 report AMS-derived emissions data of nitrate, sulfate, ammonium, and chloride elsewhere (May
185 et al., 2014). As stated in May et al. (2014), our results are potentially biased by up to a factor of
186 two due to the inherent uncertainty in our estimation of CE.

187 The AMS was mounted into National Center for Atmospheric Research GV-type aircraft
188 racks with a pressure-controlled inlet to reduce fluctuations of the pressure within the
189 aerodynamic lens (Bahreini et al., 2008). During operation, data were exclusively collected using
190 the “V-mode” of the ion time-of-flight within the mass spectrometer; since no particle time-of-
191 flight data were collected, no size-resolved information is available. AMS data were typically
192 collected with a time resolution of 6 seconds (corresponding to a distance of roughly 250-300
193 m).

194 While we obtained simultaneous measurements of gas-phase CO₂, we ~~have not corrected~~
195 ~~our data for any potential interference with the signal at m/z 44 (CO₂⁺) in the AMS.~~ utilized the
196 standard correction in the fragmentation table from Allan et al. (2004), rather than explicit
197 corrections for CO₂ to account for differences within and without of the plume. The AMS
198 samples particles roughly 10^7 times more efficiently than the gas-phase. We estimate that on
199 average, our plume OA concentrations are positively biased by $0.0044 \pm 0.0019\%$ (both near the
200 source and downwind), our background OA concentrations are positively biased by $0.025 \pm$
201 0.021% , and our m/z 44 measurements are positively biased by $0.20 \pm 0.11\%$, all based on

202 co-located gas-phase CO₂ measurements. Consequently, we deemed this correction unnecessary
203 as this interference represents < 0.5% of our reported values.

204 2.2.2. Single Particle Soot Photometer

205 The SP2 provides operationally-defined rBC mass concentrations via laser-induced
206 incandescence (Stephens et al., 2003; Schwarz et al., 2006). Absorbing material present in
207 particles is heated to its vaporization temperature and emits radiation, which is measured by
208 optical detectors. This approach removes uncertainties due to interferences of artifacts that have
209 been observed during filter-based approaches (Kirchstetter et al., 2004) and excludes the
210 influence of “brown” carbon that can bias optical absorption methods (Andreae and Gelencsér,
211 2006; Lack et al., 2012), although it has been shown the method responds to some metals. Signal
212 is related to rBC mass via calibration procedures; during SCREAM, calibrations were performed
213 using fullerene soot. Generally, rBC mass concentrations were recorded every 6 seconds, similar
214 to the AMS. Additional details related to the SP2 operation during this campaign can be found in
215 May et al. (2014).

216 2.2.3. Cavity Ring-Down Spectrometer

217 A Picarro G2401 provided ~~±0.5~~ Hz measurements of CO₂, CO, CH₄, and H₂O, which are
218 the major gas-phase emissions from combustion sources. The CRDS was calibrated in-flight
219 using mixed standards of CO₂/CO/CH₄ and procedures similar to those described by Urbanski
220 (2013). These data were applied to calculate emission ratios and emission factors of particle-
221 phase species, as described below.

222 ~~2.2.4. Airborne Fourier Transform Infrared Spectrometer~~

223 ~~—The AFTIR data used and obtained during this study are described in detail by Akagi et~~
224 ~~al. (2013). “Grab samples” were collected in background air and as the Twin Otter traversed the~~
225 ~~smoke plume; these samples were held for 2–3 minutes of signal averaging in order to improve~~

226 ~~sensitivity. Compound mixing ratios were quantified via a non-linear least squares method for~~
227 ~~the majority of the identifiable trace gases (Burling et al., 2011; Yokelson et al., 2007); however,~~
228 ~~nitrogen monoxide (NO) and nitrogen dioxide (NO₂) were quantified by integration of selected~~
229 ~~peaks in the spectra. These AFTIR data provide complementary results describing gas-phase~~
230 ~~chemistry that assist the interpretation of particle-phase measurements.~~

231 2.3. Data Processing

232 2.3.1 Plume Identification and Age

233 ~~Emissions were rapidly diluted and mixed within the boundary layer (within roughly 30~~
234 ~~min downwind), and the plumes did not penetrate into the free troposphere, so visual tracking of~~
235 ~~the plumes was challenging. Furthermore, the plume from the FJ 22b fire entered restricted air~~
236 ~~space near Columbia, SC, so it was only possible to follow this plume for a short distance from~~
237 ~~the point of emission. As discussed previously, visual plume identification was challenging.~~

238 Positive downwind plume intercepts were confirmed through simultaneous spikes in measured
239 values of OA, BC, and CO. These confirmed intercepts were corroborated by simultaneous
240 increases in smoke markers (Sullivan et al., 2014) and trace gases (Akagi et al., 2013). Intercept-
241 averaged concentrations for each transect were derived by integrating the excess area (above
242 background) under the data time series curves and dividing by the elapsed time in the window of
243 integration.

244 Sample ages (times since emission) were estimated using the distance from the source
245 and mean wind speed. Distance from the source was computed using the haversine formula and
246 the spatial coordinates measured by the AIMMS-20. Mean wind speed was also measured using
247 the AIMMS-20. Akagi et al. (2013) estimated that this approach has an uncertainty of roughly
248 30%, largely due to uncertainties in the wind speed data. Due to the ~~nature of the flight~~
249 ~~path~~plume tracking challenges, plume intercepts were rarely ~~occurred perfectly~~ perpendicular to

250 the plume; ~~in fact, they and~~ were often diagonal transects. Thus, a given sample can be
251 associated with a range of estimated d ages. In subsequent figures, we plot the average age of a
252 plume intercept along with error bars representing the range of ages; in these figures, we do not
253 include the estimated uncertainty of 30% on this range.

254 ~~This Based on the time since emission calculation we can identify provides a pseudo-~~
255 ~~Lagrangian estimate of plume samples that were emitted during the time period that we were~~
256 ~~sampling at the source and thus we have higher confidence in the initial value for these age, and~~
257 ~~hence, a downwind samples and they can be termed pseudo-Lagrangian. can be related to~~
258 ~~emissions measured directly at the source at the appropriate earlier time. Therefore, some of the~~
259 ~~data we present in figures are labeled “Lagrangian” when we had corresponding source~~
260 ~~measurements, whereas for others (labeled “non-Lagrangian”) we can estimate time since~~
261 ~~emission based on distance from the source and ambient wind speed but do not have a~~
262 ~~corresponding source samples. For consistency with May et al. (2014), we defined “near-source”~~
263 ~~samples as those collected within 5 km of the fire, while downwind samples were those collected~~
264 ~~at distances greater than 5 km.~~

265 In-plume data from all research flights were corrected for local background
266 concentrations via integration under the curves in data time series between out-of-plume
267 measurements. The resulting species concentrations are “excess” concentrations and denoted by
268 the delta symbol, i.e., ΔX is the excess concentration of species X. We show background values
269 of some parameters in some of the following figures; these background concentrations represent
270 the median background concentration for the duration of the given flight. Sample background-
271 corrected data are provided in Figure 1.

272 2.3.2. Excess Emission Ratios and Emission Factors

273 Normalized excess mixing ratios (NEMR) are often used to account for transient fire
274 behavior and the dilution and mixing of plumes with background air during transport (e.g.,
275 Hobbs et al., 2003) and are defined as:

276
$$NEMR_x = \frac{\Delta X}{\Delta CO} \quad (1)$$

277 where ΔX is the excess concentration of species X, and ΔCO is the background-corrected value
278 of CO. Since both numerator and denominator are excess quantities, uncertainties in their values
279 increase as the plume dilutes and in-plume concentrations approach the background
280 concentrations. Here, we report ~~instantaneous~~ plume-integrated $NEMR_x$ for each plume
281 interception, so our values ~~will~~ differ from the “fire-integrated” values [\(based on consideration of](#)
282 [all the plume intercepts\)](#) reported in May et al. (May et al., 2014). $NEMR_x$ are reported here in
283 units of $\mu\text{g m}^{-3} \text{ppmv-CO}^{-1}$; this value can be converted to g g-CO^{-1} by multiplying by a factor of
284 $8.7 \times 10^{-4} \text{ppmv-CO} (\mu\text{g-CO m}^{-3})^{-1}$. Strictly speaking, $NEMR_x$ is a misnomer for aerosol mass
285 concentrations, but we utilize this terminology for consistency with the vast body of prior
286 literature.

287 Time series of instantaneous $NEMR_x$ provide information on transient smoke behavior
288 (Jolleys et al., 2014). By associating instantaneous $NEMR_x$ with time since emission,
289 physicochemical transformations can be investigated, since $NEMR_x$ accounts for dilution and
290 thus should be constant with time in the absence of sources or sinks of the species X [or changes](#)
291 [in the initial emissions](#). The net formation of secondary organic aerosol (SOA) in smoke plumes
292 can be inferred from an increase in $NEMR_{OA}$ with distance downwind (Yokelson et al., 2009).
293 On the other hand, since OA emitted from biomass burning sources is semi-volatile, net

294 evaporation of particle-phase mass as dilution proceeds would appear as a decrease in NEMR_{OA}
295 (Akagi et al., 2012).

296 Emission factors (EF) are widely used descriptors of fire emissions (Ward and Radke,
297 1993; Andreae and Merlet, 2001). Their calculation relates the mass of X emitted (M_X) to the
298 mass of dry fuel consumed (M_{fuel}). In cases where the mass of fuel consumed is unknown, a
299 carbon mass balance approach can be applied, which relates the change in the concentration of X
300 relative to the background (ΔX ; $\mu\text{g m}^{-3}$) to the excess carbon concentrations (i.e., background-
301 corrected concentrations that have been converted to mg-C m^{-3}) of CO_2 , CO, total organic gases
302 (TOG = CH_4 + NMOG), and carbonaceous PM (PM_c):

$$303 \quad EF_X = \frac{M_X}{M_{fuel}} = \frac{\Delta X}{\Delta \text{CO}_2 + \Delta \text{CO} + \Delta \text{TOG} + \Delta \text{PM}_c} f_c \quad (2)$$

304 In Equation 2, the term f_c is a conversion factor representing fuel carbon content. Since we lack
305 detailed fuel information, we assume that $f_c = 0.50$, roughly the average fuel carbon content of
306 southeastern (SE) US coastal plain biomass fuels reported in laboratory studies (Burling et al.,
307 2010; May et al., 2014; McMeeking et al., 2009); ~~we also lack an estimate of~~ Since ΔTOG in the
308 ~~emissions. Furthermore, and~~ $\Delta \text{PM}_c \ll (\Delta \text{CO}_2 + \Delta \text{CO})$. ~~Hence, for convenience~~ we approximate
309 EF_X neglecting both ΔTOG and ΔPM_c , which ~~may results~~ in an over-estimate in EF_X of $\sim 3\text{-}45\%$
310 (Yokelson et al., 2013b). Like NEMR_X , EF_X are based on excess concentrations and account for
311 dilution, but if an “emission factor” is computed with downwind data, the value obtained reflects
312 ~~changes in the initial emission factor plus the effect of~~ any sources or sinks of the originally-
313 emitted species X. Hereafter, we will refer to downwind “emission factors” as “export factors”,
314 also denoted as EF_X and calculated from Equation 2; the main distinction is that an export factor
315 describes X downwind from the source, and thus, ~~except for pseudo-Lagrangian samples~~ may be

316 subject to both changes in the emissions as the fire burns and atmospheric transformations. We
317 report EF_x as g or mg kg-dry-fuel⁻¹.

318 3. Results and Discussion

319 During the study, only two fires provided adequate downwind aerosol data allowing us to
320 investigate in-plume aerosol physicochemical transformations: the FJ 9b fire and the Francis
321 Marion fire. As mentioned earlier, the plume from the FJ 22b fire entered restricted airspace and
322 could not be pursued. Further, the Georgetown fire was a small fire whose plume rapidly mixed
323 with the background, so downwind ΔOA was small and uncertain; the Bamberg samples
324 represented two distinct fuel types as shown elsewhere (May et al., 2014; Sullivan et al., 2014),
325 making it difficult to distinguish transformations during transport from differences in the
326 sources.

327 In Figure 2, we present composition data versus estimated time since emission ~~of~~for the
328 NEMR or EF ~~of~~for four major components present in the biomass burning smoke sampled for
329 the FJ 9b fire: OA (NEMR_{OA}; Figure 2a), rBC (NEMR_{rBC}; Figure 2b), CO (EF_{CO}; Figure 2c),
330 and CO₂ (EF_{CO2}; Figure 2d). Data near the source are presented as box-and-whisker plots (25th-
331 75th and 10th-90th percentiles); these data were collected ~~over~~during roughly 2.5 hours of ~~real-~~
332 time,sampling during which the modified combustion efficiency (MCE) (Ward and Radke, 1993)
333 varied between 0.900 and 0.930, which explains some of the variability in the data. Data up to
334 five hours downwind were obtained and are shown as closed symbols for Lagrangian points, or
335 open symbols for non-Lagrangian data. For downwind samples, vertical errors bars represent
336 estimated measurement uncertainties while horizontal error bars represent the range of estimated
337 plume ages for non-perpendicular plume transects; horizontal error bars do not account for the
338 estimated 30% measurement uncertainty in wind speed. To assess whether differences near the

339 source and downwind are statistically significant, we conducted unpaired t -tests. When the
340 corresponding two-tailed p value ≤ 0.05 , we consider the results to be significantly different;
341 conversely, if the p value > 0.05 , we infer that there is no significant difference.

342 We expect rBC, CO, and CO₂ to be conserved with transport since they are stable in the
343 atmosphere on the timescales considered here. Indeed, unpaired t -tests for the data shown in
344 Figures 2b-d indicate that there was no significant difference between-in the average value of
345 these species at the source and downwind (two-tailed p values > 0.13). Differences in mean
346 downwind EFs are attributable to measurement uncertainties, including identification of the
347 plume edges, and variability in the combustion phase-at the source. Based-on theFitting an
348 exponential decay with distance from the source of absolute mixing ratios of CO and CO₂, we
349 infer an average mixing rate (the inverse of the dilution timescale, or the time to decay by 1/e) of
350 1.6 hr⁻¹ during the FJ 9b experiment.

351 Since OA is reactive and semi-volatile, it is perhaps not surprising that the downwind
352 NEMR_{OA} over 2-5 hr of atmospheric aging is significantly lower than the NEMR_{OA} at the source
353 (Figure 2a; two-tailed p value = 0.015), suggesting a net loss of emitted OA via evaporation
354 and/or reaction. As demonstrated by Akagi et al. (2013), the smoke plume was photochemically
355 active, as evident through enhancements of ozone and formaldehyde relative to the source.

356 Figure 3 is identical to Figure 2 but represents the Francis Marion burn, the only other
357 case with downwind aerosol measurements adequate to assess aging downwind aerosol
358 measurements (here, up to 1.5 hr after emission) and no other known biomass burning emission
359 sources. Akagi et al. (2013) inferred photochemical processing was occurring in the Francis
360 Marion plume, based on observed downwind enhancements of ozone and formaldehyde relative
361 to the source. However, unlike the FJ 9b fire, none of the computed downwind NEMR and EF

362 shown in Fig. 3 were significantly different from the source (all two-tailed p values > 0.32). The
363 background OA concentrations, which we assume contribute to gas-particle partitioning of
364 emitted OA by providing additional absorptive material, were roughly 50% greater during the
365 Francis Marion fire compared to the FJ 9b fire; furthermore, the ~~dilution-mixing~~ rate was 20%
366 slower for the Francis Marion plume (1.3 hr^{-1}), and the plume ~~aging~~ was observed over a much
367 shorter time period. These factors would slow the evaporation of emitted OA, and limit the time
368 over which chemical transformations could occur and be observed. Indeed, over the first 1.5 hr
369 after emission, the data for FJ 9b shown in Figure 2 also indicated no statistically-significant
370 ~~detectable~~ change in NEMR_{OA} .

371 3.1. Chemical Transformations of Organic Aerosol

372 In this section, we ~~investigate chemical transformations of the organic aerosol, fragment~~
373 ~~evolution (Figure 4), and elemental ratio analyses (Figure 5)~~ ~~utilize using~~ two approaches to
374 ~~investigate chemical transformations of the organic aerosol~~ for ~~the two cases~~ ~~both fires~~ with
375 ~~adequate~~ downwind data; the FJ 9b and Francis Marion burns; ~~fragment evolution (Figure 4)~~
376 ~~and elemental ratio analyses (Figure 5)~~. ~~Both~~ Ng et al. (2010) ~~and~~ Morgan et al. (2010)
377 demonstrated that “fresh” OA in ambient samples can be distinguished by organic fragment
378 signatures in the mass spectra (e.g., C_3H_7^+ at m/z 43), while “aged” OA is more highly oxidized
379 and can be distinguished by a strong contribution of CO_2^+ (m/z 44). The fractional contributions
380 of each of these fragments to the total OA concentration (e.g., $f_{44} = C_{44}/C_{\text{OA}}$, where C_{44} is the
381 mass concentration of particulate CO_2^+ , ~~which is likely due to decarboxylation on the vaporizer~~
382 ~~surface rather than CO_2 molecules being present in the aerosol sample~~) change with atmospheric
383 aging: f_{43} is expected to decrease and f_{44} to increase.

384 However, neither Ng et al. (2010) nor Morgan et al. (2010) directly considered the
385 influence of biomass burning. Cubison et al. (2011) and Ortega et al. (2013) thus modified the
386 approach and compared f_{60} and f_{44} to infer photochemical aging of BBOA. Levoglucosan and
387 other anhydrosugars ~~that are combustion-pyrolysis~~ products of cellulose, and thus are used as
388 molecular markers for biomass burning emissions (Simoneit et al., 1999; Sullivan et al., 2008);
389 these compounds, contribute an be identified to AMS spectra at m/z 60 ($C_2H_4O_2^+$) (Alfarra et
390 al., 2007; Lee et al., 2010). May et al. (2012) and references therein demonstrated that
391 levoglucosan is semi-volatile at ambient conditions; ~~hence, and thus m/z 60 is expected to~~
392 decrease due to evaporation during dilution, if this finding is extrapolated to all ~~anhydrosugars~~
393 in general contributing species. Furthermore, Hennigan et al. (2010) demonstrated that
394 levoglucosan is reactive and chemically decays similar to the hydrocarbon-like (m/z 43)
395 fragments. Thus, f_{60} may change due to both dilution-driven evaporation and photo-oxidation
396 processes. ~~Cubison et al. (2011) and Ortega et al. (2013) thus modified the Ng et al. (2010)~~
397 ~~approach and, comparing f_{60} and f_{44} to infer photochemical aging of BBOA.~~

398 In Figure 4, we present excess f_{60} (Δf_{60}) and excess f_{44} (Δf_{44}) for the FJ 9b and Francis
399 Marion fires. These excess fragment fractional contributions were computed from background-
400 corrected m/z 60 or m/z 44 mass concentrations by dividing that excess concentration by ΔO_A .
401 Thus, as the plume dilutes and becomes less distinguishable from the background, Δf_{60} and Δf_{44}
402 should remain constant if neither preferentially evaporates, reacts, or accumulates within the
403 plume. For the FJ 9b fire, the source-downwind differences for both Δf_{60} (Figure 4a) and Δf_{44}
404 (Figure 4b) are statistically significant (two-tailed p value < 0.0001). For the Francis Marion fire,
405 Δf_{60} (Figure 4c) is significantly lower ~~at the source than~~ downwind than at the source (two-tailed
406 p value < 0.0001), while Δf_{44} (Figure 4d) is significantly higher downwind than at the source

407 (two-tailed p value = 0.029). The result for Δf_{60} is consistent with Figure 2a; that is, the decrease
408 in Δf_{60} downwind during the FJ 9b fire reflects the decrease in NEMR_{OA} . An observed decrease
409 in Δf_{60} with no decrease in OA concentration during the Francis Marion fire may be related to
410 chemical reactions of compounds that fragment to m/z 60 or to differences in the volatility of
411 these compounds compared to the bulk OA. The mechanistic driver of all transformations will be
412 explored below.

413 The increase in Δf_{44} with plume age for both fires indicates a compositional change
414 toward increasing mass fractional contributions from molecules that fragment to CO_2^+ . If only
415 dilution (and hence, evaporation) was occurring in the plumes as they moved downwind, Δf_{44}
416 should be conserved, provided its parent's volatility is similar to that of the bulk of the emitted
417 OA. The observed increase in CO_2^+ in these photochemically-active environments may indicate
418 that production of SOA occurred within the plumes, although there were no statistically-
419 significant increases in the measured downwind NEMR_{OA} , as also found in some previous field
420 studies (e.g., Capes et al., 2008; Cubison et al., 2011). On the other hand, this increase could also
421 indicate that the species fragmenting to m/z 44 are relatively less volatile than the bulk OA that
422 evaporates during transport and dilution.

423 There is experimental evidence investigating chemically-resolved volatility that is
424 consistent with the evaporation of bulk OA resulting in a relative increase in m/z 44 and a
425 relative decrease in m/z 60. Huffman et al. (2009a) demonstrated for ambient samples in two
426 different megacities that, at a given temperature in a thermodenuder, m/z 60 evaporated to a
427 greater extent than the bulk OA, while m/z 44 evaporated to a lesser extent than the bulk OA.
428 While heating OA is technically not the same as diluting OA, the response of OA to increased
429 temperature is analogous to the response of OA to increased dilution. Furthermore, Collier and

430 Zhang (2013) demonstrated that f_{44} increased with decreasing C_{OA} for vehicle test data in the
431 absence of chemistry and hypothesized that this observation was attributable to preferential
432 evaporation of less-oxidized OA species. Thus, the observed changes during SCREAM in Δf_{44}
433 and Δf_{60} may be due, at least in part, to physical changes occurring as some of the emitted OA is
434 volatilized upon dilution with ambient air.

435 Another framework for tracking the chemical evolution of OA was suggested by Heald et
436 al. (2010), who proposed the use of elemental ratios (hydrogen to carbon, H:C, and oxygen to
437 carbon, O:C) to describe photochemical aging of OA. Similar to the fragment evolution, with
438 increasing OH exposure, H:C is expected to decrease (e.g., due to hydrogen abstraction
439 reactions) and O:C is expected to increase (e.g., due to oxygen addition to alkyl radicals). In
440 Figure 5 we present the evolution of the elemental ratio of H:C and O:C during atmospheric
441 transport of the biomass burning plumes from both fires; values of the ratios for the average
442 background, out-of-plume ratio for each fire are shown as dotted lines. We assume uncertainties
443 of 31% of O:C and 10% for H:C, based on Aiken et al. (2008).

444 For both fires, the average background H:C ratio was roughly 15% greater than the H:C
445 at the source; downwind H:C values were mostly within the source variability. As the plumes
446 were transported downwind and mixed with background OA, based on measured dilution rates
447 we expected H:C to have increased toward the background values on a 2- to 3-hour timescale if
448 it were a conserved tracer. The lack of a clear ~~decrease-increase~~ with time since emission in both
449 experiments suggests either that loss of both H and C occurred in the plume, or increases in C
450 occurred without corresponding addition of H that would maintain the H:C observed at the
451 source. Typically, H:C decreases with increasing oxidation (Heald et al., 2010).

452 _____ For O:C, about half the downwind values were higher than could be explained by
453 measured variability at the source, and the background OA had O:C within (but at the lower end)
454 of the range at the source. Dilution with background air was thus expected to have had little
455 impact on O:C if O:C were a conserved tracer. Like m/z 44, O:C could have increased with time
456 if photochemical production and condensation of high O:C species or photochemical aging of
457 aerosol had occurred (Kroll et al., 2011).

458 _____ However, the observed decreases in NEMR_{OA} (whether statistically significant or not)
459 suggests that changes in H:C and O:C may potentially be induced~~or potentially~~ by a solely
460 physical process (i.e., if C were lost from the aerosol phase by~~reaction or preferential~~
461 evaporation of species that had lower O:C than the average observed at the source); ~~I~~In fact,
462 Huffman et al. (2009b) demonstrated that O:C increased and H:C decreased with increasing
463 evaporation of bulk OA in biomass burning emissions during thermodenuder experiments.

464 Hence, physical evaporative transformations may lead to observations that can potentially be
465 misinterpreted as~~are~~ may be -difficult to differentiate from chemical oxidative transformations.

467 3.2. Physical Transformations of Organic Aerosol

468 A net loss of OA due solely to dilution-driven evaporation may thus be consistent with
469 the observations in Figures 2-5. However, we note that we cannot definitively state that no
470 aerosol chemistry has occurred within the plumes as they age. In the following, we assume a
471 priori knowledge that dilution-driven evaporation dominates over chemical processing and
472 explore if the volatility distribution derived by May et al. (2013) for laboratory biomass burning
473 POA can reproduce our airborne observations. If it can, no oxidative chemistry is required to

474 ~~explain the data, although it is possible that some occurs.~~ ~~apply results obtained in prior lab~~
475 ~~studies of biomass burning emissions to simulate plume evolution to test this assumption.~~

476 Simulations representing the process of dilution alone are presented in Figure 6, which
477 shows EF_{OA} data (representing the emission factors near the source and export factors
478 downwind) as a function of the total mass concentration of observed organic aerosol (i.e., not
479 background corrected), C_{OA} , for six flights. Model curves were calculated using the following
480 equation (Donahue et al., 2006; Robinson et al., 2010):

$$481 \quad EF_{OA} = EF_{tot} \sum_i f_i \left(1 + \frac{C_i^*}{C_{OA}} \right)^{-1} \quad (3)$$

482 where i represents arbitrarily-chosen surrogate compounds defined by their saturation
483 concentration (C_i^* ; related to saturation vapor pressure through the ideal gas law), and f_i is the
484 mass fraction of each species i relative to the total emitted organics. The set of f_i and C_i^* is
485 referred to as a volatility distribution. Here, we utilize the volatility distribution for emissions
486 from open biomass burning that was proposed by May et al. (2013), which is comprised of
487 surrogate compounds representing seven logarithmically-spaced C_i^* bins. C_{OA} represents the
488 total OA concentration (emissions + background).

489 EF_{tot} is the emission factor of total organics (gas + particle phase) that are constrained by
490 the volatility distribution (here, all material between $C_i^* = 3 \times 10^{-3} \mu\text{g m}^{-3}$ and $3 \times 10^4 \mu\text{g m}^{-3}$, so
491 this is not equivalent to NMOG), and hence, contribute to gas-particle partitioning; EF_{tot} is likely
492 dominated by biomass-burning-derived organics but may include background semi-volatile
493 organic material that can partition into the particle phase due to the presence of the biomass
494 burning smoke. Values of EF_{tot} were inferred using Equation 3 with measured C_{OA} , calculated
495 EF_{OA} (from Equation 2), and the volatility distribution from May et al. (2013) as inputs for each
496 plume intercept. In Figure 6, the lines represent predictions based on the average EF_{tot} inferred

497 for each fire, while the shaded areas represent \pm one standard deviation in EF_{tot} . Values of EF_{tot}
498 ranged from roughly 2 g kg-fuel⁻¹ (Bamberg B) to 12 g kg-fuel⁻¹ (FJ 22b); both the FJ 9b and
499 Francis Marion fires had inferred EF_{tot} of roughly 6 g kg-fuel⁻¹. Equation 3 implies that EF_{OA}
500 (regardless of whether this represents an emission factor or export factor) decreases with
501 increasing dilution, due to the physical repartitioning of semi-volatile species.

502 There are some key assumptions to our use of Equation 3. We assume that the gas-
503 particle partitioning of the OA can be described using a parameterization derived for laboratory
504 fires, even though the OA in our samples has originated from prescribed fires in the field and
505 may be enhanced by background semi-volatile organics. We are also assuming that EF_{tot} is
506 constant in time for a given prescribed fire (i.e., it does not vary due to source variability, mixing
507 with background air, or atmospheric chemistry). Finally, we are inherently assuming that the
508 plume temperature is constant at 298 K, so dilution is the only process affecting gas-particle
509 partitioning. While these assumptions are not strictly true, they should not affect our conclusions
510 significantly on average.

511 Figures 6a and 6b provide EF_{OA} calculated near the source and downwind for the FJ 9b
512 and Francis Marion fires, respectively. Near-source data from the FJ 22b and Georgetown fires
513 are presented in Figure 6c, and from the Bamberg fires in Figure 6d. Generally, the near-source
514 data for all fires follow the expected trend, exhibiting a decrease in EF_{OA} with decreasing ~~plume-~~
515 integrated total measured (i.e., not background-corrected) C_{OA} , as would be expected for a semi-
516 volatile tracer with the characteristics summarized by May et al. (2013); variability in near-
517 source data arises due to proximity to the source and to the center of the plume as well as the
518 smoke production rate. Downwind data (only available for Figures 6a and 6b) also generally
519 follow the trend predicted by Equation 3; indeed, downwind OA concentrations appear to be

520 lower than predicted, suggesting evaporation of emitted OA dominates over production and
521 condensation of SOA if occurring. Performing a t-test on the inferred EF_{tot} for both the FJ 9b and
522 Francis Marion fires indicates that the differences between near-source and downwind values are
523 not statistically significant (p -value > 0.1), suggesting no observable SOA production from
524 oxidation reactions (e.g., excess OA has reached equilibrium).

525 We also note that the predictions in Figure 6 are based on a composite volatility
526 distribution that best represented biomass fuels investigated in the laboratory during the
527 FLAME-III study, which has been extrapolated to the field in this study. Also, fire behavior was
528 variable during the several hours over which data were collected, as evident in the MCE
529 variability (Akagi et al., 2013); the emissions of organics has been demonstrated to vary with
530 MCE (May et al., 2014; McMeeking et al., 2009). All data are represented using a single set of
531 model inputs, which does not account for this variability with MCE. While other factors likely
532 play a role, these two are likely to be the most important. Regardless, the differences in OA
533 observed at the source and downwind for these plumes can be explained by a simple model of
534 gas-particle partitioning.

535 4. Conclusions

536 In this work, we present field observations of the physicochemical evolution of the
537 organic aerosol present in biomass burning plumes from two prescribed fires in South Carolina.
538 Downwind observations of rBC to CO ratios and emission factors of CO, and CO₂ are not
539 statistically different on average from those at the source. The downwind ratio of OA to CO was
540 significantly lower than at the source during-for the fire that we were able to follow downwind
541 for up to five hours of atmospheric aging. ~~-, but this~~ The downwind OA to CO ratio was not

542 significantly different downwind for the other fire, which may be related to the much shorter
543 observable atmospheric aging time (~2 hr).

544 We observed significant differences in downwind ratios of AMS mass fragments thought
545 to be indicative of fresh biomass burning emissions (m/z 60, which decreased) and more oxidized
546 OA species (m/z 44, which increased), consistent with prior reported laboratory photo-oxidation
547 experiments. While the observed increases in Δf_{44} (and the O:C ratio) imply the possibility of
548 SOA production within the plume, these observed changes are also consistent with differences in
549 the volatilities of the species fragmenting to m/z 60 and m/z 44 relative to the bulk OA, resulting
550 in differences in evaporation as the plume dilutes into background air.

551 Our observations and model simulations suggest that dilution-driven evaporation out of
552 the particle phase dominated ~~ds~~ over condensation of semi-volatile material into the particle phase
553 over roughly the first two hours of transport during the FJ 9b fire. ~~after which t~~ After this, t the
554 OA in the plume reached an apparent equilibrium ~~steady-state~~ with the background in our
555 observations, as there is no net change to $NEMR_{OA}$ (i.e., there is no obvious dilution-driven
556 evaporation or SOA production); thus, OA transformation can be predicted with a simple gas-
557 particle partitioning model. For the Francis Marion fire, ~~due to limited downwind data, we~~
558 cannot draw a similar conclusion ~~for the Francis Marion fire with any certainty.~~ This finding
559 decrease in $NEMR_{OA}$ for the FJ 9b fire is consistent with results from previous literature (Akagi
560 et al., 2012; Jolleys et al., 2012, 2015); however, other studies report increases in OA with
561 increasing plume age (DeCarlo et al., 2008; Vakkari et al., 2014; Yokelson et al., 2009). The
562 exact cause of this variability in observations is unclear. These remaining unexplained
563 differences among different field studies highlight the need for additional research on
564 atmospheric physicochemical transformations of biomass burning plumes.

565 Acknowledgements

566 We acknowledge funding from the Joint Fire Science Program under project JFSP 11-1-5-12 to
567 S.M.K. and the Strategic Environmental Research and Development Program project RC-1649
568 administered partly through the Forest Service Research Joint Venture Agreement
569 08JV11272166039 to R.Y. Additional flight hours and CRDS data were provided by Joint Fire
570 Science Program project 08-1-6-09 to S.U. Adaptation of the Twin Otter was supported by NSF
571 grants ATM-0531044 and ATM-0936321 to R.Y. We also thank Ezra Levin and the NSF/NCAR
572 Research Aviation Facility for assistance with the installation of instruments to the Twin Otter;
573 Shane Murphy, Roya Bahreini, and Ann Middlebrook for guidance in modifying the CSU AMS
574 for aircraft operation; and Jose Jimenez, Tim Onasch, Jill Craven, and Misha Schurman for
575 discussions related to AMS data analysis. This work would not have been possible without the
576 support of the Twin Otter [Science-Support](#) Team, especially pilot Bill Mank and mechanic Steve
577 Woods; John Maitland and the forestry staff at Fort Jackson who conducted those prescribed
578 fires; and the Columbia Dispatch Office of the South Carolina Forestry Commission [for-who](#)
579 [providing](#) additional prescribed fire locations during the campaign.

580 5. References

- 581 Aiken, A. C., Decarlo, P. F., Kroll, J. H., Worsnop, D. R., Huffman, J. A., Docherty, K. S.,
582 Ulbrich, I. M., Mohr, C., Kimmel, J. R., Sueper, D., Sun, Y., Zhang, Q., Trimborn, A.,
583 Northway, M., Ziemann, P. J., Canagaratna, M. R., Onasch, T. B., Alfarra, M. R., Prevot, A. S.
584 H., Dommen, J., Duplissy, J., Metzger, A., Baltensperger, U. and Jimenez, J. L.: O/C and
585 OM/OC Ratios of Primary, Secondary, and Ambient Organic Aerosols with High-Resolution
586 Time-of-Flight Aerosol Mass Spectrometry, *Environ. Sci. Technol.*, 42(12), 4478–4485,
587 doi:10.1021/es703009q, 2008.
- 588 Akagi, S. K., Burling, I. R., Mendoza, A., Johnson, T. J., Cameron, M., Griffith, D. W. T., Paton-
589 Walsh, C., Weise, D. R., Reardon, J. and Yokelson, R. J.: Field measurements of trace gases
590 emitted by prescribed fires in southeastern US pine forests using an open-path FTIR system,
591 *Atmos. Chem. Phys.*, 14(1), 199–215, doi:10.5194/acp-14-199-2014, 2014.

592 Akagi, S. K., Craven, J. S., Taylor, J. W., McMeeking, G. R., Yokelson, R. J., Burling, I. R.,
593 Urbanski, S. P., Wold, C. E., Seinfeld, J. H., Coe, H., Alvarado, M. J. and Weise, D. R.:
594 Evolution of trace gases and particles emitted by a chaparral fire in California, *Atmos. Chem.*
595 *Phys.*, 12(3), 1397–1421, doi:10.5194/acp-12-1397-2012, 2012.

596 Akagi, S. K., Yokelson, R. J., Burling, I. R., Meinardi, S., Simpson, I., Blake, D. R.,
597 McMeeking, G. R., Sullivan, A., Lee, T., Kreidenweis, S., Urbanski, S., Reardon, J., Griffith, D.
598 W. T., Johnson, T. J. and Weise, D. R.: Measurements of reactive trace gases and variable O₃
599 formation rates in some South Carolina biomass burning plumes, *Atmos. Chem. Phys.*, 13(3),
600 1141–1165, doi:10.5194/acp-13-1141-2013, 2013.

601 Akagi, S. K., Yokelson, R. J., Wiedinmyer, C., Alvarado, M. J., Reid, J. S., Karl, T., Crouse, J.
602 D. and Wennberg, P. O.: Emission factors for open and domestic biomass burning for use in
603 atmospheric models, *Atmos. Chem. Phys.*, 11(9), 4039–4072, doi:10.5194/acp-11-4039-2011,
604 2011.

605 Alfarra, M. R., Prévôt, A. S. H., Szidat, S., Sandradewi, J., Weimer, S., Lanz, V. A., Schreiber,
606 D., Mohr, M. and Baltensperger, U.: Identification of the Mass Spectral Signature of Organic
607 Aerosols from Wood Burning Emissions, *Environ. Sci. Technol.*, 41(16), 5770–5777,
608 doi:10.1021/es062289b, 2007.

609 Allan, J. D., Delia, A. E., Coe, H., Bower, K. N., Alfarra, M. R., Jimenez, J. L., Middlebrook, A.
610 M., Drewnick, F., Onasch, T. B., Canagaratna, M. R., Jayne, J. T. and Worsnop, D. R.: A
611 generalised method for the extraction of chemically resolved mass spectra from Aerodyne
612 aerosol mass spectrometer data, *J. Aerosol Sci.*, 35(7), 909–922,
613 doi:10.1016/j.jaerosci.2004.02.007, 2004.

614 Andreae, M. O. and Gelencsér, A.: Black carbon or brown carbon? The nature of light-absorbing
615 carbonaceous aerosols, *Atmos. Chem. Phys.*, 6(10), 3131–3148, doi:10.5194/acp-6-3131-2006,
616 2006.

617 Andreae, M. O. and Merlet, P.: Emission of trace gases and aerosols from biomass burning,
618 *Global Biogeochem. Cycles*, 15(4), 955–966, doi:10.1029/2000GB001382, 2001.

619 Bahreini, R., Dunlea, E. J., Matthew, B. M., Simons, C., Docherty, K. S., DeCarlo, P. F.,
620 Jimenez, J. L., Brock, C. A. and Middlebrook, A. M.: Design and Operation of a Pressure-
621 Controlled Inlet for Airborne Sampling with an Aerodynamic Aerosol Lens, *Aerosol Sci.*
622 *Technol.*, 42(6), 465–471, doi:10.1080/02786820802178514, 2008.

623 Bond, T. C., Doherty, S. J., Fahey, D. W., Forster, P. M., Berntsen, T., DeAngelo, B. J., Flanner,
624 M. G., Ghan, S., Kärcher, B., Koch, D., Kinne, S., Kondo, Y., Quinn, P. K., Sarofim, M. C.,
625 Schultz, M. G., Schulz, M., Venkataraman, C., Zhang, H., Zhang, S., Bellouin, N., Guttikunda,
626 S. K., Hopke, P. K., Jacobson, M. Z., Kaiser, J. W., Klimont, Z., Lohmann, U., Schwarz, J. P.,
627 Shindell, D., Storelvmo, T., Warren, S. G. and Zender, C. S.: Bounding the role of black carbon
628 in the climate system: A scientific assessment, *J. Geophys. Res. Atmos.*, 118(11), 5380–5552,
629 doi:10.1002/jgrd.50171, 2013.

630 Burling, I. R., Yokelson, R. J., Akagi, S. K., Urbanski, S. P., Wold, C. E., Griffith, D. W. T.,
631 Johnson, T. J., Reardon, J. and Weise, D. R.: Airborne and ground-based measurements of the
632 trace gases and particles emitted by prescribed fires in the United States, *Atmos. Chem. Phys.*,
633 11(23), 12197–12216, doi:10.5194/acp-11-12197-2011, 2011.

634 Burling, I. R., Yokelson, R. J., Griffith, D. W. T., Johnson, T. J., Veres, P., Roberts, J. M.,
635 Warneke, C., Urbanski, S. P., Reardon, J., Weise, D. R., Hao, W. M. and de Gouw, J.:
636 Laboratory measurements of trace gas emissions from biomass burning of fuel types from the
637 southeastern and southwestern United States, *Atmos. Chem. Phys.*, 10(22), 11115–11130,
638 doi:10.5194/acp-10-11115-2010, 2010.

639 Capes, G., Johnson, B., McFiggans, G., Williams, P. I., Haywood, J. and Coe, H.: Aging of
640 biomass burning aerosols over West Africa: Aircraft measurements of chemical composition,
641 microphysical properties, and emission ratios, *J. Geophys. Res.*, 113, D00C15,
642 doi:10.1029/2008JD009845, 2008.

643 Christian, T. J., Kleiss, B., Yokelson, R. J., Holzinger, R., Crutzen, P. J., Hao, W. M., Saharjo, B.
644 H. and Ward, D. E.: Comprehensive laboratory measurements of biomass-burning emissions: 1.
645 Emissions from Indonesian, African, and other fuels, *J. Geophys. Res.*, 108(D23), 4719,
646 doi:10.1029/2003JD003704, 2003.

647 Collier, S. and Zhang, Q.: Gas-phase CO₂ subtraction for improved measurements of the organic
648 aerosol mass concentration and oxidation degree by an aerosol mass spectrometer., *Environ. Sci.*
649 *Technol.*, 47(24), 14324–31, doi:10.1021/es404024h, 2013.

650 Cubison, M. J., Ortega, A. M., Hayes, P. L., Farmer, D. K., Day, D., Lechner, M. J., Brune, W.
651 H., Apel, E., Diskin, G. S., Fisher, J. A., Fuelberg, H. E., Hecobian, A., Knapp, D. J., Mikoviny,
652 T., Riemer, D., Sachse, G. W., Sessions, W., Weber, R. J., Weinheimer, A. J., Wisthaler, A. and
653 Jimenez, J. L.: Effects of aging on organic aerosol from open biomass burning smoke in aircraft
654 and laboratory studies, *Atmos. Chem. Phys.*, 11(23), 12049–12064, doi:10.5194/acp-11-12049-
655 2011, 2011.

656 DeCarlo, P. F., Dunlea, E. J., Kimmel, J. R., Aiken, A. C., Sueper, D., Crouse, J., Wennberg, P.
657 O., Emmons, L., Shinozuka, Y., Clarke, A., Zhou, J., Tomlinson, J., Collins, D. R., Knapp, D.,
658 Weinheimer, A. J., Montzka, D. D., Campos, T. and Jimenez, J. L.: Fast airborne aerosol size
659 and chemistry measurements above Mexico City and Central Mexico during the MILAGRO
660 campaign, *Atmos. Chem. Phys.*, 8(14), 4027–4048, doi:10.5194/acp-8-4027-2008, 2008.

661 DeCarlo, P. F., Kimmel, J. R., Trimborn, A., Northway, M. J., Jayne, J. T., Aiken, A. C., Gonin,
662 M., Fuhrer, K., Horvath, T., Docherty, K. S., Worsnop, D. R. and Jimenez, J. L.: Field-
663 deployable, high-resolution, time-of-flight aerosol mass spectrometer., *Anal. Chem.*, 78(24),
664 8281–9, doi:10.1021/ac061249n, 2006.

665 Donahue, N. M., Chuang, W., Epstein, S. A., Kroll, J. H., Worsnop, D. R., Robinson, A. L.,
666 Adams, P. J. and Pandis, S. N.: Why do organic aerosols exist? Understanding aerosol lifetimes

667 using the two-dimensional volatility basis set, *Environ. Chem.*, 10(3), 151,
668 doi:10.1071/EN13022, 2013.

669 Heald, C. L., Kroll, J. H., Jimenez, J. L., Docherty, K. S., DeCarlo, P. F., Aiken, A. C., Chen, Q.,
670 Martin, S. T., Farmer, D. K. and Artaxo, P.: A simplified description of the evolution of organic
671 aerosol composition in the atmosphere, *Geophys. Res. Lett.*, 37(8), L08803,
672 doi:10.1029/2010GL042737, 2010.

673 Heilman, W. E., Liu, Y., Urbanski, S., Kovalev, V. and Mickler, R.: Wildland fire emissions,
674 carbon, and climate: Plume rise, atmospheric transport, and chemistry processes, *For. Ecol.
675 Manage.*, 317, 70–79, doi:10.1016/j.foreco.2013.02.001, 2014.

676 Hennigan, C. J., Miracolo, M. A., Engelhart, G. J., May, A. A., Presto, A. A., Lee, T., Sullivan,
677 A. P., McMeeking, G. R., Coe, H., Wold, C. E., Hao, W.-M., Gilman, J. B., Kuster, W. C., de
678 Gouw, J., Schichtel, B. A., Kreidenweis, S. M. and Robinson, A. L.: Chemical and physical
679 transformations of organic aerosol from the photo-oxidation of open biomass burning emissions
680 in an environmental chamber, *Atmos. Chem. Phys.*, 11(15), 7669–7686, doi:10.5194/acp-11-
681 7669-2011, 2011.

682 Hennigan, C. J., Sullivan, A. P., Collett, J. L. and Robinson, A. L.: Levoglucosan stability in
683 biomass burning particles exposed to hydroxyl radicals, *Geophys. Res. Lett.*, 37(9), n/a–n/a,
684 doi:10.1029/2010GL043088, 2010.

685 Hobbs, P. V., Sinha, P., Yokelson, R. J., Christian, T. J., Blake, D. R., Gao, S., Kirchstetter, T.
686 W., Novakov, T. and Pilewskie, P.: Evolution of gases and particles from a savanna fire in South
687 Africa, *J. Geophys. Res.*, 108(D13), 8485, doi:10.1029/2002JD002352, 2003.

688 Hosseini, S., Urbanski, S. P., Dixit, P., Qi, L., Burling, I. R., Yokelson, R. J., Johnson, T. J.,
689 Shrivastava, M., Jung, H. S., Weise, D. R., Miller, J. W. and Cocker, D. R.: Laboratory
690 characterization of PM emissions from combustion of wildland biomass fuels, *J. Geophys. Res.*
691 *Atmos.*, 118(17), 9914–9929, doi:10.1002/jgrd.50481, 2013.

692 Huffman, J. A., Docherty, K. S., Aiken, A. C., Cubison, M. J., Ulbrich, I. M., DeCarlo, P. F.,
693 Sueper, D., Jayne, J. T., Worsnop, D. R., Ziemann, P. J. and Jimenez, J. L.: Chemically-resolved
694 aerosol volatility measurements from two megacity field studies, *Atmos. Chem. Phys.*, 9(18),
695 7161–7182, doi:10.5194/acp-9-7161-2009, 2009a.

696 Huffman, J. A., Docherty, K. S., Mohr, C., Cubison, M. J., Ulbrich, I. M., Ziemann, P. J.,
697 Onasch, T. B. and Jimenez, J. L.: Chemically-Resolved Volatility Measurements of Organic
698 Aerosol from Different Sources, *Environ. Sci. Technol.*, 43(14), 5351–5357,
699 doi:10.1021/es803539d, 2009b.

700 Jolleys, M. D., Coe, H., McFiggans, G., Capes, G., Allan, J. D., Crosier, J., Williams, P. I.,
701 Allen, G., Bower, K. N., Jimenez, J. L., Russell, L. M., Grutter, M. and Baumgardner, D.:
702 Characterizing the aging of biomass burning organic aerosol by use of mixing ratios: a meta-

703 analysis of four regions., *Environ. Sci. Technol.*, 46(24), 13093–102, doi:10.1021/es302386v,
704 2012.

705 Jolleys, M. D., Coe, H., McFiggans, G., McMeeking, G. R., Lee, T., Kreidenweis, S. M., Collett,
706 J. L. and Sullivan, A. P.: Organic aerosol emission ratios from the laboratory combustion of
707 biomass fuels, *J. Geophys. Res. Atmos.*, 119(22), 12,850–12,871, doi:10.1002/2014JD021589,
708 2014.

709 Jolleys, M. D., Coe, H., Mcfiggans, G., Taylor, J. W., Shea, S. J. O., Breton, M. Le, Bauguitte, S.
710 J., Moller, S., Carlo, P. Di, Aruffo, E., Palmer, P. I., Lee, J. D., Percival, C. J. and Gallagher, M.
711 W.: Properties and evolution of biomass burning organic aerosol from Canadian boreal forest
712 fires, *Atmos. Chem. Phys.*, 15(6), 3077–3095, doi:10.5194/acp-15-3077-2015, 2015.

713 Kirchstetter, T. W., Novakov, T. and Hobbs, P. V.: Evidence that the spectral dependence of
714 light absorption by aerosols is affected by organic carbon, *J. Geophys. Res.*, 109(D21), D21208,
715 doi:10.1029/2004JD004999, 2004.

716 Kroll, J. H., Donahue, N. M., Jimenez, J. L., Kessler, S. H., Canagaratna, M. R., Wilson, K. R.,
717 Altieri, K. E., Mazzoleni, L. R., Wozniak, A. S., Bluhm, H., Mysak, E. R., Smith, J. D., Kolb, C.
718 E. and Worsnop, D. R.: Carbon oxidation state as a metric for describing the chemistry of
719 atmospheric organic aerosol., *Nat. Chem.*, 3(2), 133–9, doi:10.1038/nchem.948, 2011.

720 Lack, D. A., Langridge, J. M., Bahreini, R., Cappa, C. D., Middlebrook, A. M. and Schwarz, J.
721 P.: Brown carbon and internal mixing in biomass burning particles., *Proc. Natl. Acad. Sci. U. S.*
722 *A.*, 109(37), 14802–7, doi:10.1073/pnas.1206575109, 2012.

723 Lee, T., Sullivan, A. P., Mack, L., Jimenez, J. L., Kreidenweis, S. M., Onasch, T. B., Worsnop,
724 D. R., Malm, W., Wold, C. E., Hao, W. M. and Collett, J. L.: Chemical Smoke Marker
725 Emissions During Flaming and Smoldering Phases of Laboratory Open Burning of Wildland
726 Fuels, *Aerosol Sci. Technol.*, 44(9), i–v, doi:10.1080/02786826.2010.499884, 2010.

727 Marple, V. A., Rubow, K. L. and Behm, S. M.: A Microorifice Uniform Deposit Impactor
728 (MOUDI): Description, Calibration, and Use, *Aerosol Sci. Technol.*, 14(4), 434–446,
729 doi:10.1080/02786829108959504, 1991.

730 May, A. A., Levin, E. J. T., Hennigan, C. J., Riipinen, I., Lee, T., Collett, J. L., Jimenez, J. L.,
731 Kreidenweis, S. M. and Robinson, A. L.: Gas-particle partitioning of primary organic aerosol
732 emissions: 3. Biomass burning, *J. Geophys. Res. Atmos.*, 118(19), 11,327–11,338,
733 doi:10.1002/jgrd.50828, 2013.

734 May, A. A., McMeeking, G. R., Lee, T., Taylor, J. W., Craven, J. S., Burling, I., Sullivan, A. P.,
735 Akagi, S., Collett, J. L., Flynn, M., Coe, H., Urbanski, S. P., Seinfeld, J. H., Yokelson, R. J. and
736 Kreidenweis, S. M.: Aerosol emissions from prescribed fires in the United States: A synthesis of
737 laboratory and aircraft measurements, *J. Geophys. Res. Atmos.*, 119(20), 11,826–11,849,
738 doi:10.1002/2014JD021848, 2014.

- 739 May, A. A., Saleh, R., Hennigan, C. J., Donahue, N. M. and Robinson, A. L.: Volatility of
740 organic molecular markers used for source apportionment analysis: measurements and
741 implications for atmospheric lifetime., *Environ. Sci. Technol.*, 46(22), 12435–44,
742 doi:10.1021/es302276t, 2012.
- 743 McMeeking, G. R., Kreidenweis, S. M., Baker, S., Carrico, C. M., Chow, J. C., Collett, J. L.,
744 Hao, W. M., Holden, A. S., Kirchstetter, T. W., Malm, W. C., Moosmüller, H., Sullivan, A. P.
745 and Wold, C. E.: Emissions of trace gases and aerosols during the open combustion of biomass
746 in the laboratory, *J. Geophys. Res.*, 114(D19), D19210, doi:10.1029/2009JD011836, 2009.
- 747 Middlebrook, A. M., Bahreini, R., Jimenez, J. L. and Canagaratna, M. R.: Evaluation of
748 Composition-Dependent Collection Efficiencies for the Aerodyne Aerosol Mass Spectrometer
749 using Field Data, *Aerosol Sci. Technol.*, 46(3), 258–271, doi:10.1080/02786826.2011.620041,
750 2012.
- 751 Morgan, W. T., Allan, J. D., Bower, K. N., Highwood, E. J., Liu, D., McMeeking, G. R.,
752 Northway, M. J., Williams, P. I., Krejci, R. and Coe, H.: Airborne measurements of the spatial
753 distribution of aerosol chemical composition across Europe and evolution of the organic fraction,
754 *Atmos. Chem. Phys.*, 10(8), 4065–4083, doi:10.5194/acp-10-4065-2010, 2010.
- 755 Ng, N. L., Canagaratna, M. R., Zhang, Q., Jimenez, J. L., Tian, J., Ulbrich, I. M., Kroll, J. H.,
756 Docherty, K. S., Chhabra, P. S., Bahreini, R., Murphy, S. M., Seinfeld, J. H., Hildebrandt, L.,
757 Donahue, N. M., DeCarlo, P. F., Lanz, V. A., Prévôt, A. S. H., Dinar, E., Rudich, Y. and
758 Worsnop, D. R.: Organic aerosol components observed in Northern Hemispheric datasets from
759 Aerosol Mass Spectrometry, *Atmos. Chem. Phys.*, 10(10), 4625–4641, doi:10.5194/acp-10-
760 4625-2010, 2010.
- 761 Ortega, A. M., Day, D. A., Cubison, M. J., Brune, W. H., Bon, D., de Gouw, J. A. and Jimenez,
762 J. L.: Secondary organic aerosol formation and primary organic aerosol oxidation from biomass-
763 burning smoke in a flow reactor during FLAME-3, *Atmos. Chem. Phys.*, 13(22), 11551–11571,
764 doi:10.5194/acp-13-11551-2013, 2013.
- 765 Reid, J. S., Koppmann, R., Eck, T. F. and Eleuterio, D. P.: A review of biomass burning
766 emissions part II: intensive physical properties of biomass burning particles, *Atmos. Chem.*
767 *Phys.*, 5(3), 799–825, doi:10.5194/acp-5-799-2005, 2005.
- 768 Robinson, A. L., Grieshop, A. P., Donahue, N. M. and Hunt, S. W.: Updating the Conceptual
769 Model for Fine Particle Mass Emissions from Combustion Systems, *J. Air Waste Manage.*
770 *Assoc.*, 60(10), 1204–1222, doi:10.3155/1047-3289.60.10.1204, 2010.
- 771 Schwarz, J. P., Gao, R. S., Fahey, D. W., Thomson, D. S., Watts, L. A., Wilson, J. C., Reeves, J.
772 M., Darbeheshti, M., Baumgardner, D. G., Kok, G. L., Chung, S. H., Schulz, M., Hendricks, J.,
773 Lauer, A., Kärcher, B., Slowik, J. G., Rosenlof, K. H., Thompson, T. L., Langford, A. O.,
774 Loewenstein, M. and Aikin, K. C.: Single-particle measurements of midlatitude black carbon and
775 light-scattering aerosols from the boundary layer to the lower stratosphere, *J. Geophys. Res.*
776 *Atmos.*, 111(16), D16207, doi:10.1029/2006JD007076, 2006.

777 Simoneit, B. R. T., Schauer, J. J., Nolte, C. G., Oros, D. R., Elias, V. O., Fraser, M. P., Rogge,
778 W. F. and Cass, G. R.: Levoglucosan, a tracer for cellulose in biomass burning and atmospheric
779 particles, *Atmos. Environ.*, 33(2), 173–182, doi:10.1016/S1352-2310(98)00145-9, 1999.

780 Stephens, M., Turner, N. and Sandberg, J.: Particle Identification by Laser-Induced
781 Incandescence in a Solid-State Laser Cavity, *Appl. Opt.*, 42(19), 3726,
782 doi:10.1364/AO.42.003726, 2003.

783 Sueper, D., DeCarlo, P. F., Aiken, A. C. and Jimenez, J. L.: ToF-AMS High Resolution Analysis
784 Software, [online] Available from: [http://cires.colorado.edu/jimenez-group/wiki/index.php/ToF-](http://cires.colorado.edu/jimenez-group/wiki/index.php/ToF-AMS_Analysis_Software)
785 [AMS_Analysis_Software](http://cires.colorado.edu/jimenez-group/wiki/index.php/ToF-AMS_Analysis_Software), 2013.

786 Sullivan, A. P., Holden, A. S., Patterson, L. A., McMeeking, G. R., Kreidenweis, S. M., Malm,
787 W. C., Hao, W. M., Wold, C. E. and Collett, J. L.: A method for smoke marker measurements
788 and its potential application for determining the contribution of biomass burning from wildfires
789 and prescribed fires to ambient PM 2.5 organic carbon, *J. Geophys. Res.*, 113(D22), D22302,
790 doi:10.1029/2008JD010216, 2008.

791 Sullivan, A. P., May, A. A., Lee, T., McMeeking, G. R., Kreidenweis, S. M., Akagi, S. K.,
792 Yokelson, R. J., Urbanski, S. P. and Collett Jr., J. L.: Airborne characterization of smoke marker
793 ratios from prescribed burning, *Atmos. Chem. Phys.*, 14(19), 10535–10545, doi:10.5194/acp-14-
794 10535-2014, 2014.

795 Urbanski, S. P.: Combustion efficiency and emission factors for wildfire-season fires in mixed
796 conifer forests of the northern Rocky Mountains, US, *Atmos. Chem. Phys.*, 13(14), 7241–7262,
797 doi:10.5194/acp-13-7241-2013, 2013.

798 Urbanski, S. P., Hao, W. M. and Nordgren, B.: The wildland fire emission inventory: western
799 United States emission estimates and an evaluation of uncertainty, *Atmos. Chem. Phys.*, 11(24),
800 12973–13000, doi:10.5194/acp-11-12973-2011, 2011.

801 Vakkari, V., Kerminen, V.-M., Beukes, J. P., Tiitta, P., van Zyl, P. G., Josipovic, M., Venter, A.
802 D., Jaars, K., Worsnop, D. R., Kulmala, M. and Laakso, L.: Rapid changes in biomass burning
803 aerosols by atmospheric oxidation, *Geophys. Res. Lett.*, 41(7), 2644–2651,
804 doi:10.1002/2014GL059396, 2014.

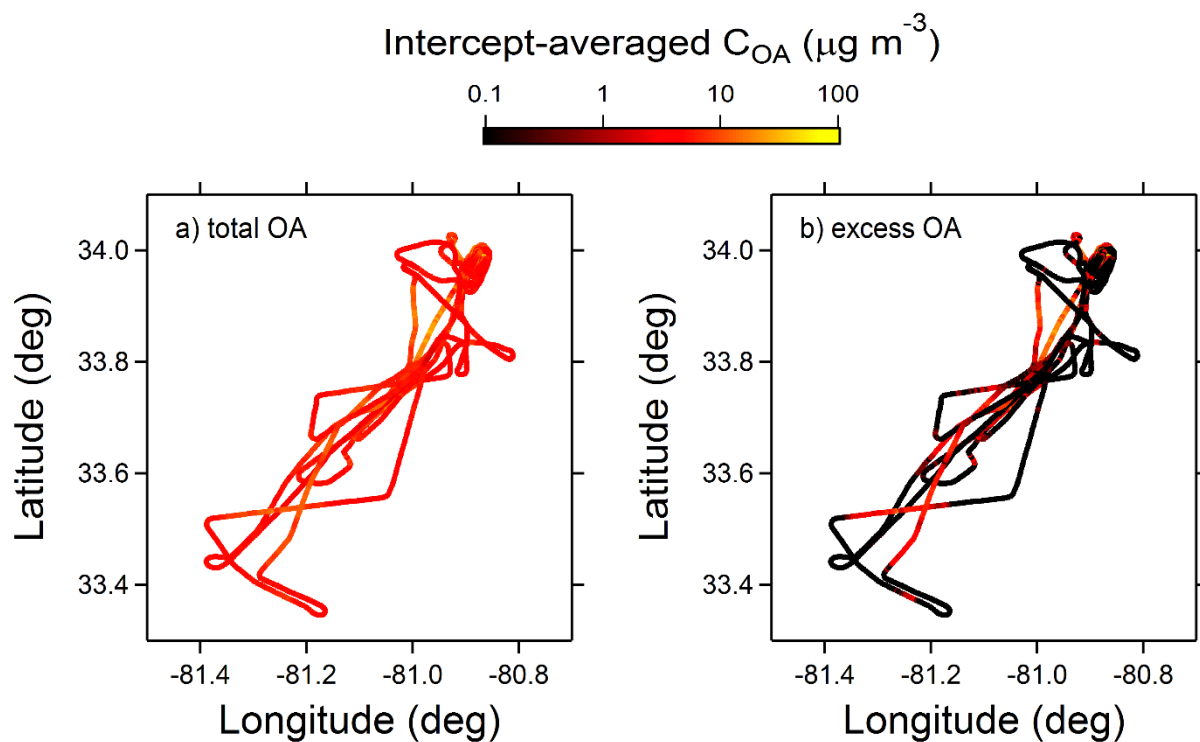
805 Ward, D. E. and Radke, L. F.: Emissions measurements from vegetation fires: A comparative
806 evaluation of methods and results, in *Fire in the Environment: The Ecological, Atmospheric, and*
807 *Climatic Importance of Vegetation Fires*, edited by P. J. Crutzen and J. G. Goldammer, pp. 53–
808 76, John Wiley & Sons, Inc., Chichester, England., 1993.

809 Watson, J. G., Chow, J. C., Chen, L.-W. A., Lowenthal, D. H., Fujita, E. M., Kuhns, H. D.,
810 Sodeman, D. A., Campbell, D. E., Moosmüller, H., Zhu, D. and Motallebi, N.: Particulate
811 emission factors for mobile fossil fuel and biomass combustion sources., *Sci. Total Environ.*,
812 409(12), 2384–96, doi:10.1016/j.scitotenv.2011.02.041, 2011.

- 813 Van der Werf, G. R., Randerson, J. T., Giglio, L., Collatz, G. J., Mu, M., Kasibhatla, P. S.,
814 Morton, D. C., DeFries, R. S., Jin, Y. and van Leeuwen, T. T.: Global fire emissions and the
815 contribution of deforestation, savanna, forest, agricultural, and peat fires (1997–2009), *Atmos.*
816 *Chem. Phys.*, 10(23), 11707–11735, doi:10.5194/acp-10-11707-2010, 2010.
- 817 Wiedinmyer, C., Akagi, S. K., Yokelson, R. J., Emmons, L. K., Al-Saadi, J. A., Orlando, J. J.
818 and Soja, A. J.: The Fire INventory from NCAR (FINN): a high resolution global model to
819 estimate the emissions from open burning, *Geosci. Model Dev.*, 4(3), 625–641,
820 doi:10.5194/gmd-4-625-2011, 2011.
- 821 Wiedinmyer, C., Quayle, B., Geron, C., Belote, A., McKenzie, D., Zhang, X., O’Neill, S. and
822 Wynne, K. K.: Estimating emissions from fires in North America for air quality modeling,
823 *Atmos. Environ.*, 40(19), 3419–3432, doi:10.1016/j.atmosenv.2006.02.010, 2006.
- 824 Wilson, J. C., Lafleu, B. G., Hilbert, H., Seebaugh, W. R., Fox, J., Gesler, D. W., Brock, C. A.,
825 Huebert, B. J. and Mullen, J.: Function and Performance of a Low Turbulence Inlet for Sampling
826 Supermicron Particles from Aircraft Platforms, *Aerosol Sci. Technol.*, 38(8), 790–802,
827 doi:10.1080/027868290500841, 2004.
- 828 Yokelson, R. J., Burling, I. R., Gilman, J. B., Warneke, C., Stockwell, C. E., de Gouw, J., Akagi,
829 S. K., Urbanski, S. P., Veres, P., Roberts, J. M., Kuster, W. C., Reardon, J., Griffith, D. W. T.,
830 Johnson, T. J., Hosseini, S., Miller, J. W., Cocker III, D. R., Jung, H. and Weise, D. R.: Coupling
831 field and laboratory measurements to estimate the emission factors of identified and unidentified
832 trace gases for prescribed fires, *Atmos. Chem. Phys.*, 13(1), 89–116, doi:10.5194/acp-13-89-
833 2013, 2013a.
- 834 Yokelson, R. J., Burling, I. R., Gilman, J. B., Warneke, C., Stockwell, C. E., de Gouw, J., Akagi,
835 S. K., Urbanski, S. P., Veres, P., Roberts, J. M., Kuster, W. C., Reardon, J., Griffith, D. W. T.,
836 Johnson, T. J., Hosseini, S., Miller, J. W., Cocker III, D. R., Jung, H. and Weise, D. R.: Coupling
837 field and laboratory measurements to estimate the emission factors of identified and unidentified
838 trace gases for prescribed fires, *Atmos. Chem. Phys.*, 13(1), 89–116, doi:10.5194/acp-13-89-
839 2013, 2013b.
- 840 Yokelson, R. J., Crouse, J. D., DeCarlo, P. F., Karl, T., Urbanski, S., Atlas, E., Campos, T.,
841 Shinozuka, Y., Kapustin, V., Clarke, A. D., Weinheimer, A., Knapp, D. J., Montzka, D. D.,
842 Holloway, J., Weibring, P., Flocke, F., Zheng, W., Toohey, D., Wennberg, P. O., Wiedinmyer,
843 C., Mauldin, L., Fried, A., Richter, D., Walega, J., Jimenez, J. L., Adachi, K., Buseck, P. R.,
844 Hall, S. R. and Shetter, R.: Emissions from biomass burning in the Yucatan, *Atmos. Chem.*
845 *Phys.*, 9(15), 5785–5812, doi:10.5194/acp-9-5785-2009, 2009.

846

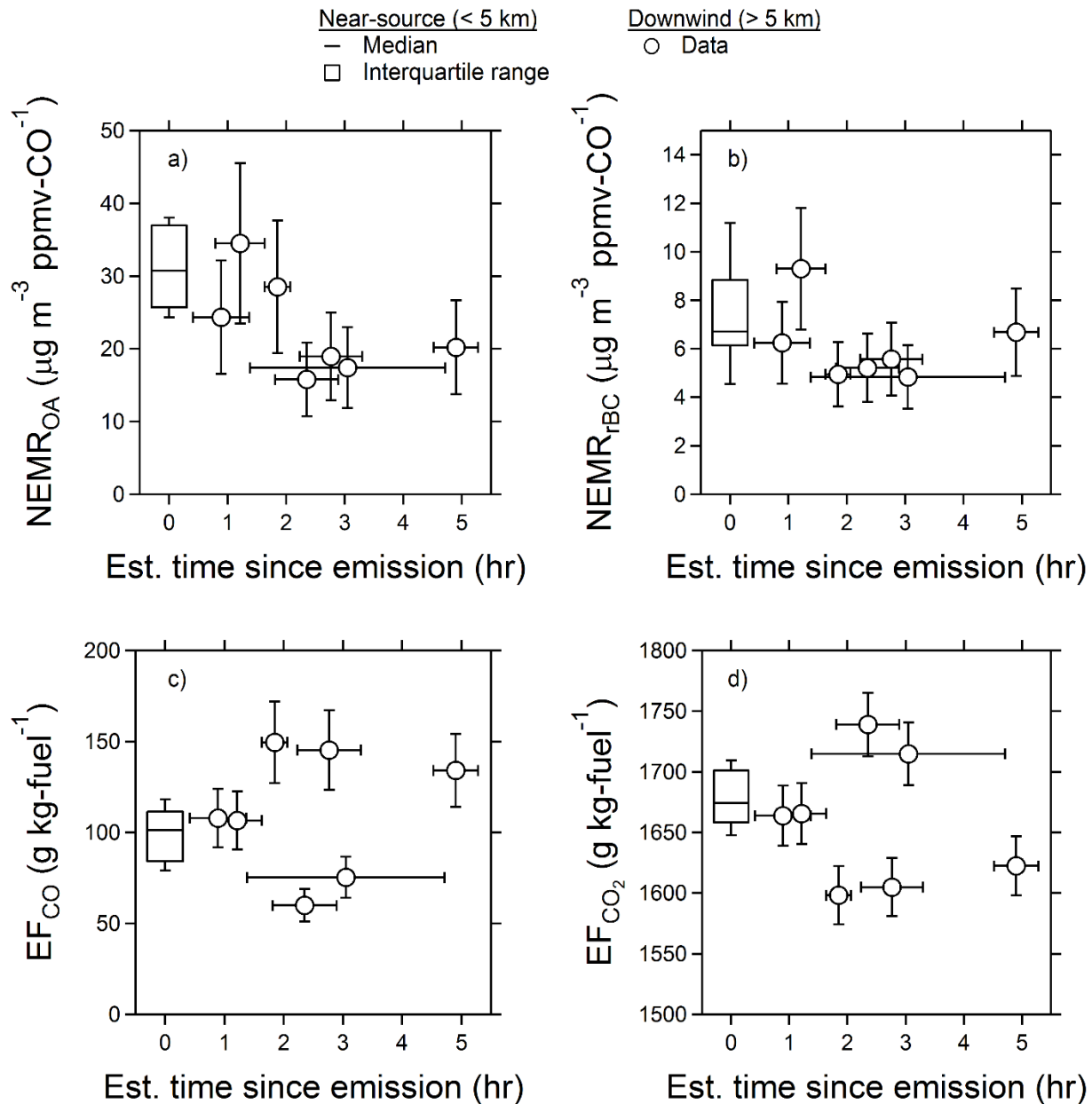
847



849

850 Figure 1.

851 Flight tracks colored by **a)** total OA concentration and **b)** excess OA concentration. Due to the
852 log-scaling of intercept-averaged concentrations, the minimum value in panel b) is set to $0.1 \mu\text{g m}^{-3}$
853 m^{-3} . Removing the background OA elucidates distinct plume transport to the southwest.



854

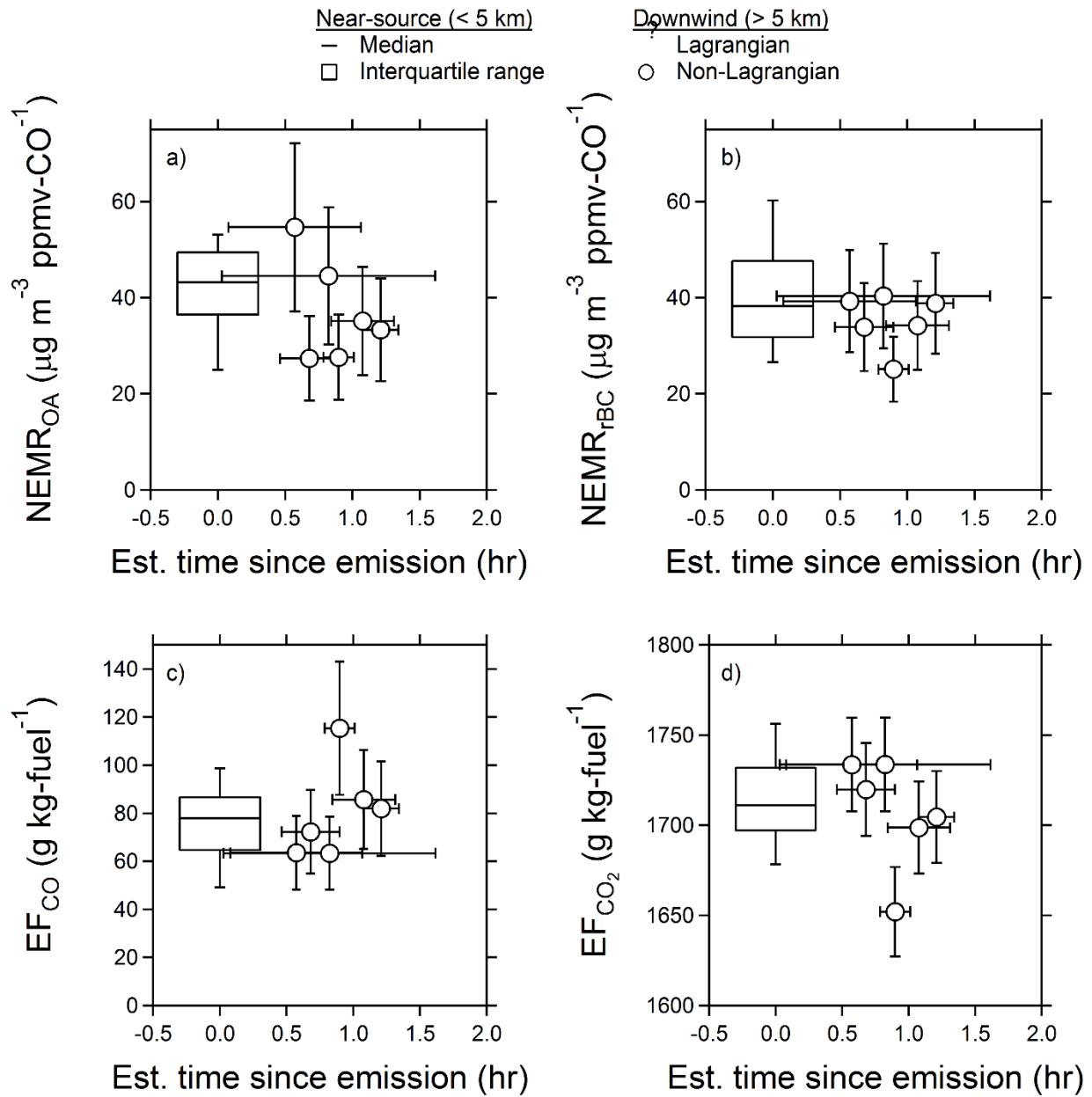
855 **Figure 2.**

856 Near-source and downwind data collected during the FJ 9b prescribed fire. **a)** the ratio of excess
 857 OA to CO; **b)** the ratio of excess rBC to CO; **c)** emission/export factor for CO; and **d)**
 858 emission/export factor of CO₂. Near-source data are represented by box-and-whisker plots
 859 (boxes: 25th and 75th percentiles; whiskers: 10th and 90th percentiles; horizontal lines: median)
 860 while downwind data are represented by markers (closed markers: Lagrangian data; open
 861 markers: non-Lagrangian data). Error bars associated with the markers indicate range of
 862 estimated time since emission (x-direction) and measurement uncertainty (y-direction). Error
 863 bars in x direction do not account for estimated 30% accuracy of windspeed.

864

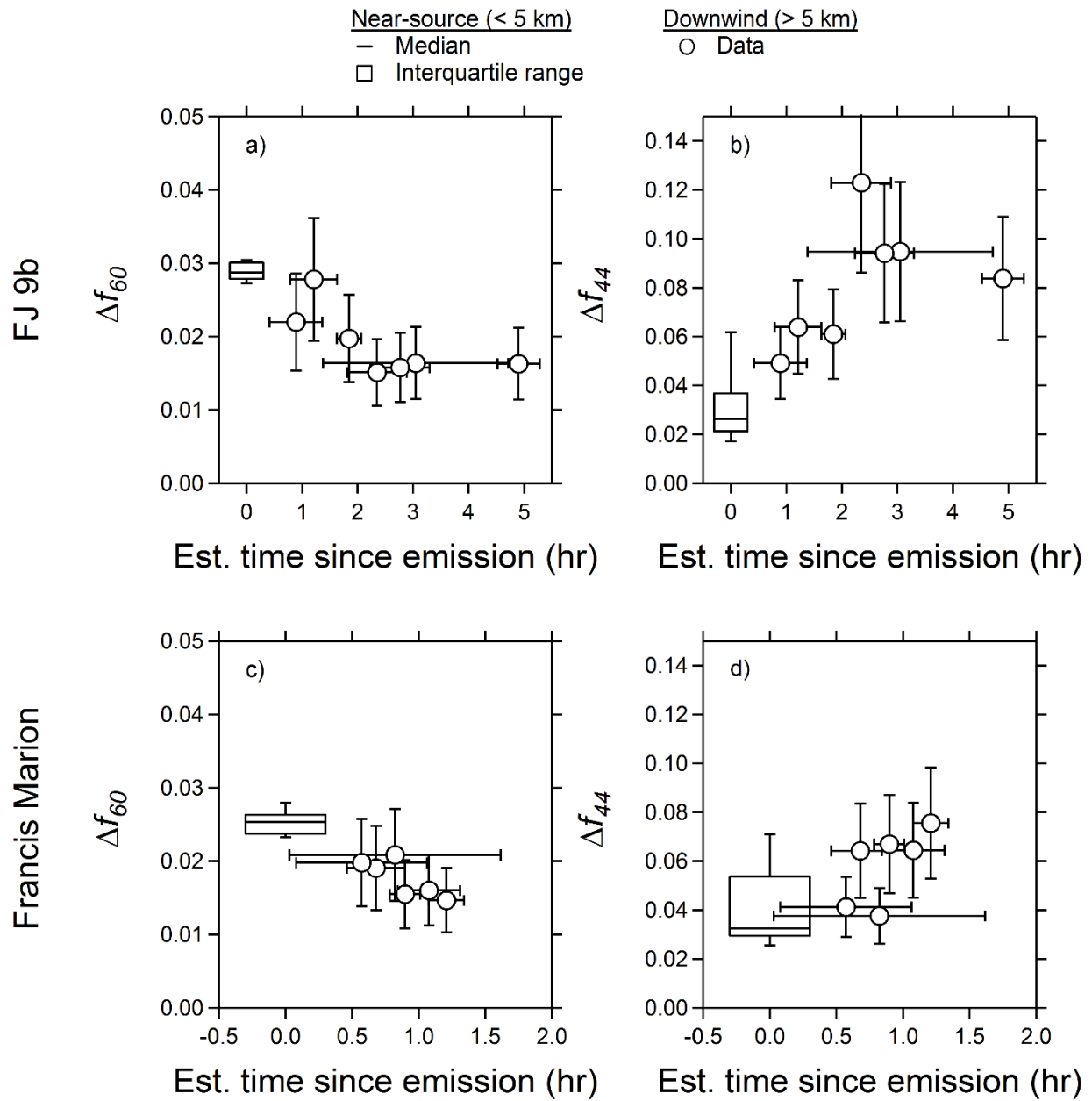
865

866



867

868 **Figure 3.**
 869 As in Figure 2, but for the Francis Marion prescribed fire.
 870



871

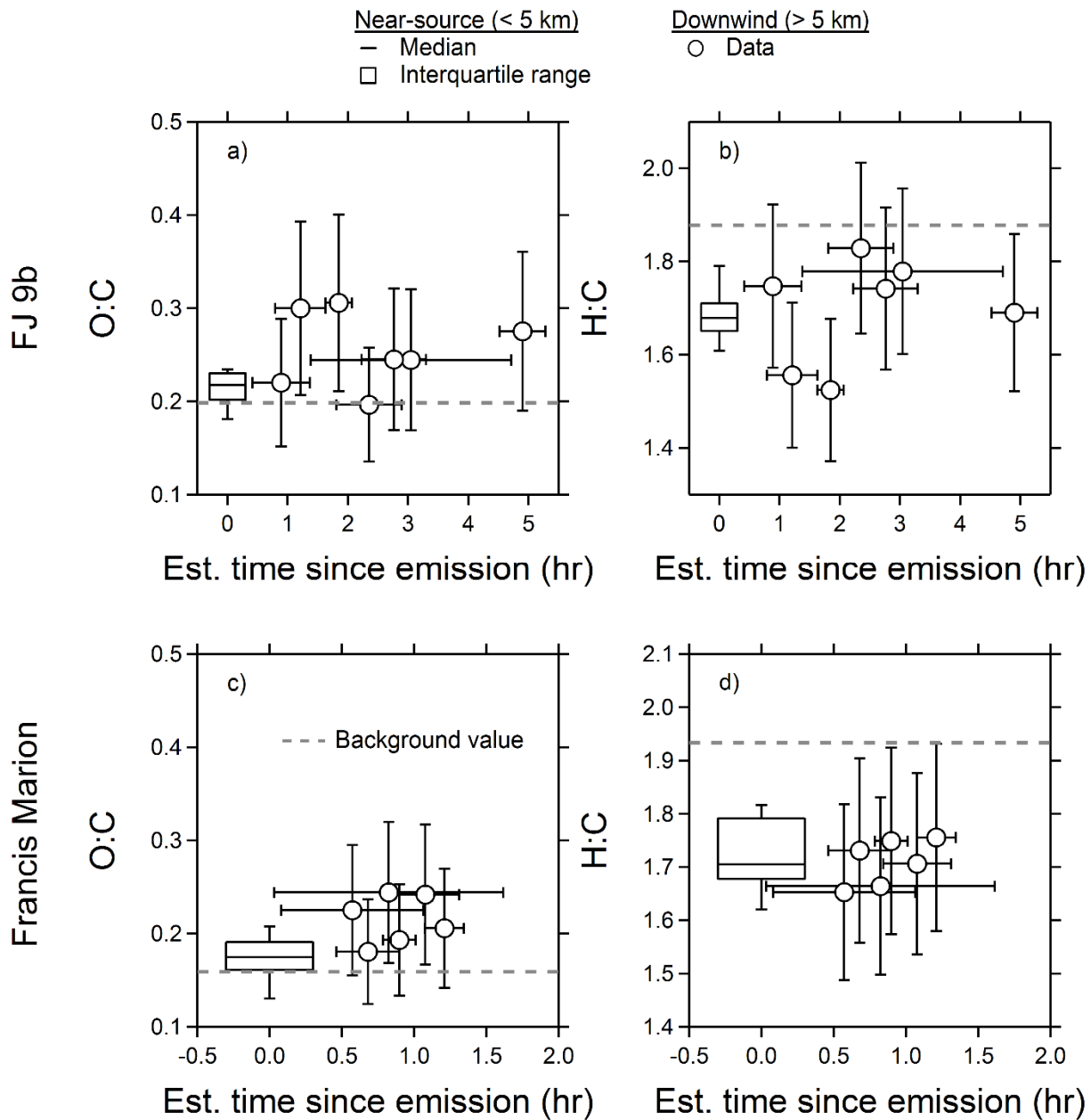
872 **Figure 4.**

873 Evolution of background-corrected AMS mass fractions. **a)** Δf_{60} for the FJ 9b fire; **b)** Δf_{44} for the
 874 FJ 9b fire; **c)** Δf_{60} for the Francis Marion fire; **d)** Δf_{44} for the Francis Marion fire. In all panels,
 875 there is a statistically-significant difference between data collected near the source and
 876 downwind. Box-and-whisker plots and markers are identical to those in Figures 2 and 3.

877

878

879
880



881

882

Figure 5.

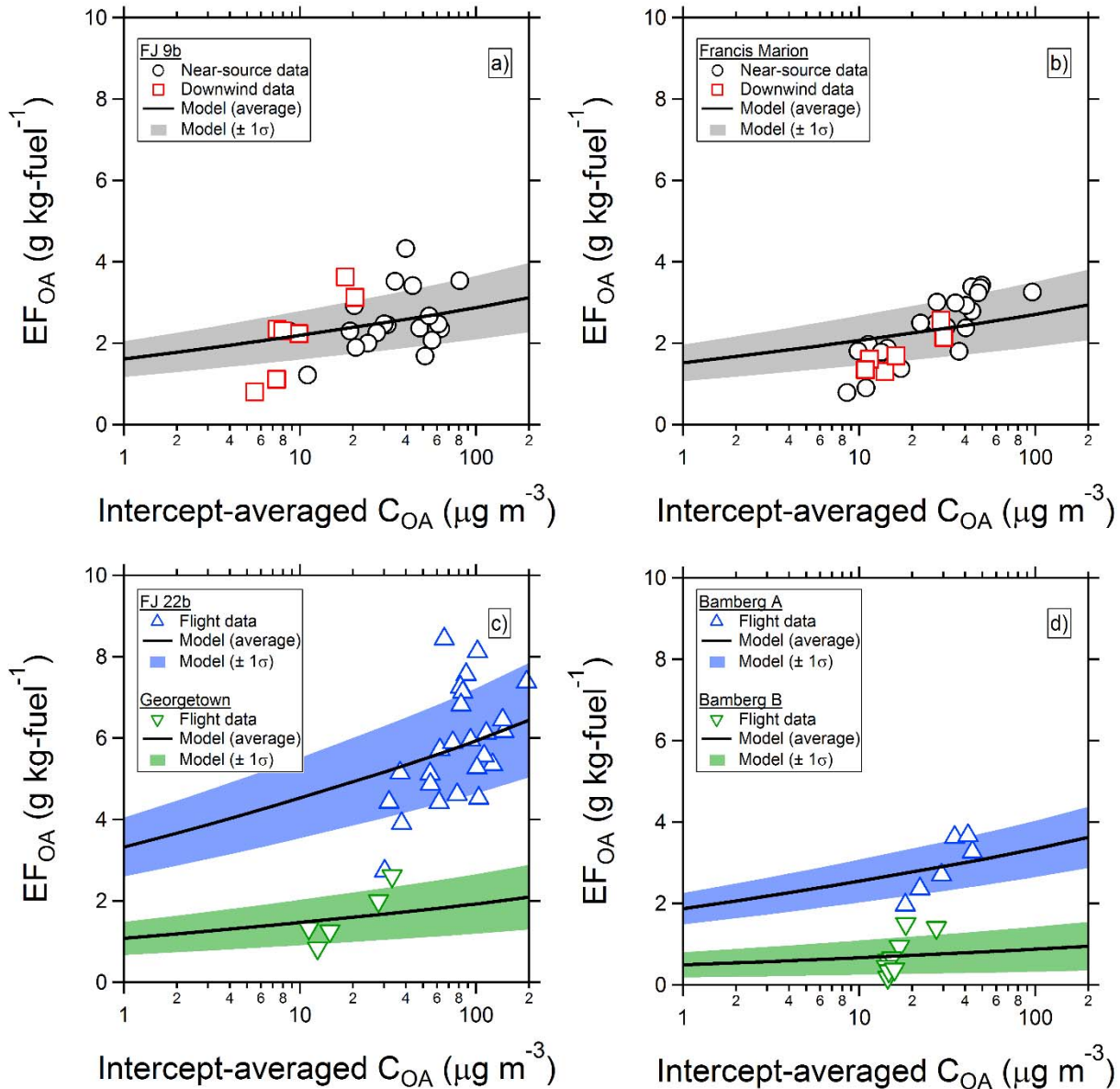
883

Evolution of elemental ratios derived from AMS data. **a)** O:C for the FJ 9b fire; **b)** H:C for the FJ 9b fire; **c)** O:C for the Francis Marion fire; **d)** H:C for the Francis Marion fire. For both fires, changes in O:C with increasing estimated time since emission are statistically significant. Dashed line is the value of the parameter in the background measurements outside of plume penetrations. Box-and-whisker plots and markers are identical to those in Figures 2 and 3.

886

887

888



891
892
893
894
895
896
897
898
899
900

Figure 6.

Changes in the emission factor of excess OA due to gas-particle partitioning as a function of total observed OA. **a)** near-source (circles) and downwind (squares) data for the FJ 9b fire; **b)** near-source (circles) and downwind (squares) data for the Francis Marion fire; **c)** near-source data for the FJ 22b (upward-facing triangles) and Georgetown (downward-facing triangles) fires; and **d)** near-source data for the two fires attributed to the Bamberg site (“A”: upward-facing triangles; “B”: downward-facing triangles). Curves represent predictions using the laboratory parameterization from May et al. (2013).